

# Planck constraints on single-field inflation

Shinji Tsujikawa,<sup>1</sup> Junko Ohashi,<sup>1</sup> Sachiko Kuroyanagi,<sup>1</sup> and Antonio De Felice<sup>2,3</sup>

<sup>1</sup>*Department of Physics, Faculty of Science, Tokyo University of Science,  
1-3, Kagurazaka, Shinjuku-ku, Tokyo 162-8601, Japan*

<sup>2</sup>*TPTP & NEP, The Institute for Fundamental Study,  
Naresuan University, Phitsanulok 65000, Thailand*

<sup>3</sup>*Thailand Center of Excellence in Physics, Ministry of Education, Bangkok 10400, Thailand*

(Dated: March 19, 2019)

We place observational constraints on slow-variation single-field inflationary models by carrying out the cosmological Monte Carlo simulation with the recent data of Planck combined with the WMAP large-angle polarization, baryon acoustic oscillations, and ACT/SPT temperature data. Our analysis covers a wide variety of models with second-order equations of motion— including potential-driven slow-roll inflation, non-minimally coupled models, running kinetic couplings, Brans-Dicke theories, potential-driven Galileon inflation, field-derivative couplings to the Einstein tensor, and k-inflation. In the presence of running kinetic exponential couplings, covariant Galileon terms, and field-derivative couplings, the tensor-to-scalar ratio of the self-coupling potential  $V(\phi) = \lambda\phi^4/4$  gets smaller relative to that in standard slow-roll inflation, but the models lie outside the  $1\sigma$  observational contour. We also show that k-inflation models can be tightly constrained by adding the bounds from the scalar non-Gaussianities. The small-field inflationary models with asymptotic flat Einstein-frame potentials in the regime  $\phi \gg M_{\text{Pl}}$  generally fit the data very well. These include the models such as Kähler-moduli inflation, non-minimally coupled Higgs inflation, and inflation in Brans-Dicke theories in the presence of the potential  $V(\phi) = 3M^2(\phi - M_{\text{Pl}})^2/4$  with the Brans-Dicke parameter  $\omega_{\text{BD}} \lesssim \mathcal{O}(1)$  (which covers the Starobinsky's model  $f(R) = R + R^2/(6M^2)$  as a special case).

## I. INTRODUCTION

Inflation is an elegant idea to resolve the horizon, flatness, and monopole problems plagued in standard big bang cosmology [1, 2]. The simplest inflationary scenario is based on a single scalar field (called inflaton) with a nearly flat potential [3–6] (see Refs. [7] for reviews). The quantum fluctuations of inflaton can be responsible for the temperature anisotropies observed in the Cosmic Microwave Background (CMB). The slow-roll single-field inflationary models predict nearly scale-invariant density perturbations [8], whose property is consistent with the CMB anisotropies measured by COBE [9] and WMAP [10].

Recently, the Planck mission released the high-precision data of CMB temperature anisotropies up to the multipoles  $\ell \lesssim 2500$  [11]. The Planck data, combined with the WMAP large-angle polarization (WP) measurement [12], showed that the spectral index  $n_s$  of curvature perturbations is constrained to be  $n_s = 0.9603 \pm 0.0073$  at the wave number  $k_0 = 0.002 \text{ Mpc}^{-1}$  [13]. The exact scale-invariance ( $n_s = 1$ ) is ruled out at more than  $5\sigma$  confidence level (CL). The tensor-to-scalar ratio  $r$  is bounded to be  $r < 0.11$  (95 % CL) at  $k_0 = 0.002 \text{ Mpc}^{-1}$ . These constraints are powerful to discriminate between a host of inflationary models (see Refs. [14] for observational constraints on particular models after the data release of Planck).

The non-Gaussianities of curvature perturbations provide additional information to break the degeneracy between models [15–18]. In the context of single-field slow-variation inflationary models, the non-linear estimator  $f_{\text{NL}}^{\text{local}}$  in the squeezed limit is as small as the orders of slow-variation parameters [18–22]. The WMAP9 data showed that the models with purely Gaussian perturbations of the local shape ( $f_{\text{NL}}^{\text{local}} = 0$ ) are outside the 68 % CL observational contour [23]. However, the more high-precision Planck data constrained the non-linear estimator to be  $f_{\text{NL}}^{\text{local}} = 2.7 \pm 5.8$  (68 % CL) [24], which means that single-field slow-variation inflationary models are consistent with the data. The non-linear parameters of equilateral and orthogonal shapes are bounded to be  $f_{\text{NL}}^{\text{equil}} = -42 \pm 75$  and  $f_{\text{NL}}^{\text{ortho}} = -25 \pm 39$  (68 % CL) from the Planck measurement. This information is useful to constrain models with the small scalar propagation speed  $c_s$  (such as k-inflation [25, 26], Galileons [27, 28], and effective field theory of inflation [29, 30]), because  $|f_{\text{NL}}^{\text{equil}}|$  and  $|f_{\text{NL}}^{\text{ortho}}|$  can be much larger than 1 in those models [20, 31–38].

In the light of Planck data, we put observational constraints on slow-variation single-field inflationary models based on the Horndeski's most general scalar-tensor theories [39–41] by running the Cosmological Monte-Carlo (CosmoMC) code [42]. The Lagrangian of the Horndeski's theories is constructed to keep the field equations of motion up to second order for avoiding the Ostrogradski instability [43]. This Lagrangian covers a wide variety of gravitational theories with one scalar degree of freedom— such as standard slow-roll inflation [3–6], non-minimally coupled models [44–46], running kinetic couplings [47, 48], Brans-Dicke theories [49] (including  $f(R)$  gravity [1]), Galileon inflation [50–52], field derivative couplings to gravity [53, 54], and k-inflation [25, 26]. For the inflationary scenarios based on

the Horndeski's theories, the power spectra and the non-Gaussianities of scalar and tensor perturbations have been already derived in Refs. [37, 38, 55, 56]. We apply those results to concrete models of inflation mentioned above.

In order to compare theoretical predictions of  $n_s$  and  $r$  with observations, we run the CosmoMC code with the latest data of Planck [11], WP [12], Baryon Acoustic Oscillations (BAO) [57–59], and ACT/SPT temperature data of high multipoles (high- $\ell$ ) [60, 61]. Since the consistency relation between the tensor-to-scalar ratio  $r$  and the tensor spectral index  $n_t$  is generally different depending on the models, we need to be careful to implement this information properly in the likelihood analysis. Apart from the cases of Galileons and k-inflation, however, the consistency relation for the models mentioned above is the same as that of standard inflation ( $r = -8n_t$ ). In k-inflation, we study the power-law inflationary scenario based on the dilatonic ghost condensate [25, 62] and Dirac-Born-Infeld (DBI) [63, 64] models. In this case, the inflationary observables can be expressed in terms of the scalar propagation speed  $c_s$  [65]. This property is useful to place further bounds on  $c_s$  from the information of scalar non-Gaussianities.

This paper is organized as follows. In Sec. II, we present the background equations of motion in the Horndeski's theories and introduce the slow-variation parameters on the quasi de-Sitter background. We also review the formulas of scalar and tensor power spectra as well as the scalar non-Gaussianities. In Sec. III, we classify inflationary models and evaluate a number of observables in each model. In Sec. IV, we carry out the likelihood analysis to test for each inflationary model with the latest observational data. Sec. V is devoted to conclusions.

## II. HORNDESKI'S THEORIES AND THE PERTURBATIONS GENERATED DURING INFLATION

We start with the action of the most general scalar-tensor theories with second-order equation of motion [39–41, 55]

$$\mathcal{S} = \int d^4x \sqrt{-g} \left[ \frac{M_{\text{pl}}^2}{2} R + P(\phi, X) - G_3(\phi, X) \square\phi + \mathcal{L}_4 + \mathcal{L}_5 \right], \quad (1)$$

where  $g$  is the determinant of the metric tensor  $g_{\mu\nu}$ ,  $M_{\text{pl}}$  is the reduced Planck mass,  $R$  is the Ricci scalar, and

$$\mathcal{L}_4 = G_4(\phi, X) R + G_{4,X} [(\square\phi)^2 - (\nabla_\mu \nabla_\nu \phi) (\nabla^\mu \nabla^\nu \phi)], \quad (2)$$

$$\mathcal{L}_5 = G_5(\phi, X) G_{\mu\nu} (\nabla^\mu \nabla^\nu \phi) - \frac{1}{6} G_{5,X} [(\square\phi)^3 - 3(\square\phi) (\nabla_\mu \nabla_\nu \phi) (\nabla^\mu \nabla^\nu \phi) + 2(\nabla^\mu \nabla_\alpha \phi) (\nabla^\alpha \nabla_\beta \phi) (\nabla^\beta \nabla_\mu \phi)]. \quad (3)$$

$P$  and  $G_i$ 's ( $i = 3, 4, 5$ ) are functions in terms of  $\phi$  and  $X = -\partial^\mu \phi \partial_\mu \phi / 2$  with the partial derivatives  $G_{i,X} \equiv \partial G_i / \partial X$ , and  $G_{\mu\nu} = R_{\mu\nu} - g_{\mu\nu} R / 2$  is the Einstein tensor ( $R_{\mu\nu}$  is the Ricci tensor).

On the flat Friedmann-Lemaître-Robertson-Walker background with the scale factor  $a(t)$  ( $t$  is cosmic time), the field equations of motion are given by [22, 35, 37, 55]

$$3M_{\text{pl}}^2 H^2 F = P_{,X} \dot{\phi}^2 - P - (G_{3,\phi} - 12H^2 G_{4,X} + 9H^2 G_{5,\phi}) \dot{\phi}^2 - 6H G_{4,\phi} \dot{\phi} - (6G_{4,\phi X} - 3G_{3,X} - 5G_{5,X} H^2) H \dot{\phi}^3 - 3(G_{5,\phi X} - 2G_{4,XX}) H^2 \dot{\phi}^4 + H^3 G_{5,XX} \dot{\phi}^5, \quad (4)$$

$$(1 - 4\delta_{G4X} - 2\delta_{G5X} + 2\delta_{G5\phi})\epsilon = \delta_{PX} + 3\delta_{G3X} - 2\delta_{G3\phi} + 6\delta_{G4X} - \delta_{G4\phi} - 6\delta_{G5\phi} + 3\delta_{G5X} + 12\delta_{G4XX} + 2\delta_{G5XX} - 10\delta_{G4\phi X} + 2\delta_{G4\phi\phi} - 8\delta_{G5\phi X} + 2\delta_{G5\phi\phi} - \delta_\phi(\delta_{G3X} + 4\delta_{G4X} - \delta_{G4\phi} + 8\delta_{G4XX} + 3\delta_{G5X} - 4\delta_{G5\phi} + 2\delta_{G5XX} - 2\delta_{G4\phi X} - 4\delta_{G5\phi X}), \quad (5)$$

where  $H = \dot{a}/a$  is the Hubble parameter (a dot represents a derivative with respect to  $t$ ),

$$F = 1 + 2G_4/M_{\text{pl}}^2, \quad (6)$$

and

$$\begin{aligned} \epsilon &= -\frac{\dot{H}}{H^2}, \quad \delta_\phi = \frac{\ddot{\phi}}{H\dot{\phi}}, \quad \delta_{PX} = \frac{P_{,XX}}{M_{\text{pl}}^2 H^2 F}, \quad \delta_{G3X} = \frac{G_{3,XX}}{M_{\text{pl}}^2 H F}, \quad \delta_{G3\phi} = \frac{G_{3,\phi X}}{M_{\text{pl}}^2 H^2 F}, \quad \delta_{G4X} = \frac{G_{4,XX}}{M_{\text{pl}}^2 F}, \\ \delta_{G4\phi} &= \frac{G_{4,\phi X}}{M_{\text{pl}}^2 H F}, \quad \delta_{G4\phi X} = \frac{G_{4,\phi XX}}{M_{\text{pl}}^2 H F}, \quad \delta_{G4\phi\phi} = \frac{G_{4,\phi\phi X}}{M_{\text{pl}}^2 H^2 F}, \quad \delta_{G4XX} = \frac{G_{4,XXX}}{M_{\text{pl}}^2 F}, \quad \delta_{G5\phi} = \frac{G_{5,\phi X}}{M_{\text{pl}}^2 F}, \\ \delta_{G5X} &= \frac{G_{5,XX}}{M_{\text{pl}}^2 F}, \quad \delta_{G5XX} = \frac{G_{5,XXX}}{M_{\text{pl}}^2 F}, \quad \delta_{G5\phi X} = \frac{G_{5,\phi XX}}{M_{\text{pl}}^2 F}, \quad \delta_{G5\phi\phi} = \frac{G_{5,\phi\phi X}}{M_{\text{pl}}^2 H F}. \end{aligned} \quad (7)$$

In order to realize the condition  $\epsilon \ll 1$ , we require that all the parameters defined in Eq. (7) are much smaller than 1. Taking the time derivative of the quantity  $\delta_{G3X}$ , we obtain

$$\eta_{G3X} \equiv \frac{\dot{\delta}_{G3X}}{H\delta_{G3X}} = \frac{2\delta_\phi \delta_{G3XX}}{\delta_{G3X}} + \frac{2\delta_{G3\phi X}}{\delta_{G3X}} + 3\delta_\phi + \epsilon - \delta_F, \quad (8)$$

where  $\delta_{G3XX} = G_{3,XX}\dot{\phi}X^2/(M_{\text{pl}}^2HF)$ ,  $\delta_{G3\phi X} = G_{3,\phi X}X^2/(M_{\text{pl}}^2H^2F)$  and  $\delta_F = \dot{F}/(HF)$ . Equation (8) shows that the quantity  $\delta_{G3\phi X}$  is second order of  $\epsilon$ . Likewise, we find

$$\{\delta_{G3\phi X}, \delta_{G3\phi\phi}, \delta_{G4\phi X}, \delta_{G4\phi\phi}, \delta_{G5\phi X}, \delta_{G5\phi\phi}\} = \mathcal{O}(\epsilon^2), \quad (9)$$

where  $\delta_{G3\phi\phi} = G_{3,\phi\phi}\dot{\phi}X/(M_{\text{pl}}^2H^3F)$ . From Eq. (5), it follows that

$$\epsilon = \delta_{PX} + 3\delta_{G3X} - 2\delta_{G3\phi} + 6\delta_{G4X} - \delta_{G4\phi} - 6\delta_{G5\phi} + 3\delta_{G5X} + 12\delta_{G4XX} + 2\delta_{G5XX} + \mathcal{O}(\epsilon^2). \quad (10)$$

The parameter  $\delta_F$  is related to  $\delta_{G4\phi}$  via

$$\delta_F = 2\delta_{G4\phi} + \mathcal{O}(\epsilon^2). \quad (11)$$

For later convenience, we define the number of e-foldings as  $N(t) = \ln a(t_f)/a(t)$ , where  $a(t)$  and  $a(t_f)$  are the scale factors at time  $t$  during inflation and at the end of inflation respectively. Since  $dN/dt = -H(t)$ , it follows that

$$N(t) = - \int_{t_f}^t H(\tilde{t}) d\tilde{t}. \quad (12)$$

The field value  $\phi_f$  at the end of inflation is known by solving  $\epsilon(\phi_f) = 1$ . The number of e-foldings when the perturbations relevant to the CMB temperature anisotropies crossed the Hubble radius is in the range  $50 < N < 60$  [13, 66].

In order to evaluate the  $n$ -point correlation functions of scalar and tensor perturbations ( $n = 2, 3$ ), it is convenient to choose the ADM metric [67] about the flat Friedmann-Lemaître-Robertson-Walker background

$$ds^2 = -[(1 + \alpha)^2 - a^{-2}(t)e^{-2\mathcal{R}}(\partial\psi)^2] dt^2 + 2\partial_i\psi dt dx^i + a^2(t)(e^{2\mathcal{R}}\delta_{ij} + h_{ij}) dx^i dx^j, \quad (13)$$

where  $\alpha, \psi, \mathcal{R}$  are scalar perturbations, and  $h_{ij}$  is the tensor perturbation. The uniform-field gauge ( $\delta\phi = 0$ ) is chosen to fix the time component of a gauge-transformation vector  $\xi^\mu$ . The scalar perturbation  $E_{,ij}$  appearing in the metric (13) is gauged away to fix the spatial component of  $\xi^\mu$ .

The linear perturbation equations can be derived by expanding the action (1) up to second order of perturbations. From the momentum and Hamiltonian constraints, the scalar perturbations  $\alpha$  and  $\psi$  are related to the curvature perturbation  $\mathcal{R}$ . Then, we obtain the second-order action of  $\mathcal{R}$ , as [37, 38, 55]

$$S_s^{(2)} = \int dt d^3x a^3 Q_s \left[ \dot{\mathcal{R}}^2 - \frac{c_s^2}{a^2} (\partial\mathcal{R})^2 \right]. \quad (14)$$

The quantities  $Q_s$  and  $c_s^2$  are defined by

$$Q_s \equiv \frac{w_1(4w_1w_3 + 9w_2^2)}{3w_2^2}, \quad (15)$$

$$c_s^2 \equiv \frac{3(2w_1^2w_2H - w_2^2w_4 + 4w_1\dot{w}_1w_2 - 2w_1^2\dot{w}_2)}{w_1(4w_1w_3 + 9w_2^2)}, \quad (16)$$

where

$$w_1 = M_{\text{pl}}^2 F(1 - 4\delta_{G4X} - 2\delta_{G5X} + 2\delta_{G5\phi}), \quad (17)$$

$$w_2 = 2M_{\text{pl}}^2 HF(1 - \delta_{G3X} - 8\delta_{G4X} - 8\delta_{G4XX} + \delta_{G4\phi} + 2\delta_{G4\phi X} - 5\delta_{G5X} - 2\delta_{G5XX} + 6\delta_{G5\phi} + 4\delta_{G5\phi X}), \quad (18)$$

$$w_3 = -9M_{\text{pl}}^2 H^2 F(1 - \delta_{PX}/3 - 2\delta_{PXX}/3 - 4\delta_{G3X} - 2\delta_{G3XX} + 2\delta_{G3\phi}/3 + 2\delta_{G3\phi X}/3 - 14\delta_{G4X} - 32\delta_{G4XX} - 8\delta_{G4XX} + 2\delta_{G4\phi} + 10\delta_{G4\phi X} + 4\delta_{G4\phi XX} - 10\delta_{G5X} - 26\delta_{G5XX}/3 - 4\delta_{G5XX}/3 + 12\delta_{G5\phi} + 18\delta_{G5\phi X} + 4\delta_{G5\phi XX}), \quad (19)$$

$$w_4 = M_{\text{pl}}^2 F(1 - 2\delta_{G5\phi} - 2\delta_{G5X}\delta_\phi), \quad (20)$$

and

$$\begin{aligned} \delta_{PXX} &= \frac{X^2 P_{,XX}}{M_{\text{pl}}^2 H^2 F}, \quad \delta_{G4XX} = \frac{G_{4,XXX} X^3}{M_{\text{pl}}^2 F}, \quad \delta_{G4\phi XX} = \frac{G_{4,\phi XX} \dot{\phi} X^2}{M_{\text{pl}}^2 HF}, \\ \delta_{G5XX} &= \frac{G_{5,XXX} H \dot{\phi} X^3}{M_{\text{pl}}^2 F}, \quad \delta_{G5\phi XX} = \frac{G_{5,\phi XX} X^3}{M_{\text{pl}}^2 F}. \end{aligned} \quad (21)$$

The terms  $\delta_{G4\phi XX}$  and  $\delta_{G5\phi XX}$  are of the order of  $\epsilon^2$ .

At leading order in slow-variation parameters, we have

$$Q_s = M_{\text{pl}}^2 F q_s, \quad (22)$$

$$q_s \equiv \delta_{PX} + 2\delta_{PXX} + 6\delta_{G3X} + 6\delta_{G3XX} + 6\delta_{G4X} + 48\delta_{G4XX} + 24\delta_{G4XXX} \\ + 6\delta_{G5X} + 14\delta_{G5XX} + 4\delta_{G5XXX} - 2\delta_{G3\phi} - 6\delta_{G5\phi}, \quad (23)$$

$$\epsilon_s \equiv \frac{Q_s c_s^2}{M_{\text{pl}}^2 F} = \delta_{PX} + 4\delta_{G3X} + 6\delta_{G4X} + 20\delta_{G4XX} + 4\delta_{G5X} + 4\delta_{G5XX} - 2\delta_{G3\phi} - 6\delta_{G5\phi}, \quad (24)$$

by which the scalar propagation speed squared can be expressed as

$$c_s^2 = \frac{\epsilon_s}{q_s}. \quad (25)$$

The power spectrum of curvature perturbations is given by [37, 38, 55]

$$\mathcal{P}_{\mathcal{R}} = \frac{H^2}{8\pi^2 M_{\text{pl}}^2 \epsilon_s F c_s} \Big|_{c_s k = aH}, \quad (26)$$

which should be evaluated at the epoch when the mode with a wave number  $k$  crossed  $c_s k = aH$  during inflation. The scalar spectral index reads

$$n_s - 1 \equiv \frac{d \ln \mathcal{P}_{\mathcal{R}}}{d \ln k} \Big|_{c_s k = aH} = -2\epsilon - \eta_s - \delta_F - s, \quad (27)$$

where

$$\eta_s \equiv \frac{\dot{\epsilon}_s}{H \epsilon_s}, \quad s \equiv \frac{\dot{c}_s}{H c_s}. \quad (28)$$

The running spectral index is defined by

$$\alpha_s \equiv \frac{dn_s}{d \ln k} \Big|_{c_s k = aH}, \quad (29)$$

which is of the order of  $\epsilon^2$  from Eq. (27).

The transverse and traceless tensor perturbation  $h_{ij}$  can be decomposed into two independent polarization modes, as  $h_{ij} = h_+ e_{ij}^+ + h_\times e_{ij}^\times$ . The tensors  $e_{ij}^\lambda$  (where  $\lambda = +, \times$ ) satisfy the relations  $e_{ij}^+(\mathbf{k}) e_{ij}^+(-\mathbf{k})^* = 2$ ,  $e_{ij}^\times(\mathbf{k}) e_{ij}^\times(-\mathbf{k})^* = 2$ , and  $e_{ij}^+(\mathbf{k}) e_{ij}^\times(-\mathbf{k})^* = 0$  in Fourier space. The second-order action for the tensor perturbation is [37, 38, 55]

$$\mathcal{S}_t^{(2)} = \sum_{\lambda=+, \times} \int dt d^3x a^3 Q_t \left[ \dot{h}_\lambda^2 - \frac{c_t^2}{a^2} (\partial h_\lambda)^2 \right], \quad (30)$$

where

$$Q_t = \frac{1}{4} w_1 = \frac{1}{4} M_{\text{pl}}^2 F (1 - 4\delta_{G4X} - 2\delta_{G5X} + 2\delta_{G5\phi}), \quad (31)$$

$$c_t^2 = \frac{w_4}{w_1} = 1 + 4\delta_{G4X} + 2\delta_{G5X} - 4\delta_{G5\phi} + \mathcal{O}(\epsilon^2). \quad (32)$$

The tensor power spectrum reads

$$\mathcal{P}_h = \frac{H^2}{2\pi^2 Q_t c_t^3} \Big|_{c_t k = aH} \simeq \frac{2H^2}{\pi^2 M_{\text{pl}}^2 F} \Big|_{k = aH}, \quad (33)$$

where, in the second approximate equality, we have taken leading-order terms.

When both  $\mathcal{R}$  and  $h_\lambda$  approach approximately constant values during inflation, the tensor-to-scalar ratio can be evaluated as

$$r = \frac{\mathcal{P}_h}{\mathcal{P}_{\mathcal{R}}} \simeq 16 c_s \epsilon_s. \quad (34)$$

We define the tensor spectral index and its running, as

$$n_t \equiv \left. \frac{d \ln \mathcal{P}_h}{d \ln k} \right|_{k=aH} = -2\epsilon - \delta_F, \quad (35)$$

$$\alpha_t \equiv \left. \frac{dn_t}{d \ln k} \right|_{k=aH}, \quad (36)$$

where  $\alpha_t$  is of the order of  $\epsilon^2$ . Using Eqs. (10), (11), and (24), we obtain the following consistency relation

$$r = -8c_s (n_t - 2\delta_{G3X} - 16\delta_{G4XX} - 2\delta_{G5X} - 4\delta_{G5XX}) . \quad (37)$$

In order to avoid ghosts and Laplacian instabilities, we require the conditions  $Q_s > 0$ ,  $c_s^2 > 0$ ,  $Q_t > 0$ , and  $c_t^2 > 0$ , i.e.,

$$F > 0, \quad q_s > 0, \quad \epsilon_s > 0. \quad (38)$$

We focus on the models in which these conditions are satisfied.

The non-Gaussianities of curvature perturbations generated in the Horndeski's theories were evaluated in Refs. [22, 37, 38]. The bispectrum  $\mathcal{A}_{\mathcal{R}}$  is related to the three-point correlation function of  $\mathcal{R}$ , as

$$\langle \mathcal{R}(\mathbf{k}_1) \mathcal{R}(\mathbf{k}_2) \mathcal{R}(\mathbf{k}_3) \rangle = (2\pi)^7 \delta^{(3)}(\mathbf{k}_1 + \mathbf{k}_2 + \mathbf{k}_3) (\mathcal{P}_{\mathcal{R}})^2 \frac{\mathcal{A}_{\mathcal{R}}(k_1, k_2, k_3)}{\prod_{i=1}^3 k_i^3}. \quad (39)$$

We also define the non-linear estimator  $f_{\text{NL}}$ , as

$$f_{\text{NL}} = \frac{10}{3} \frac{\mathcal{A}_{\mathcal{R}}}{\sum_{i=1}^3 k_i^3}. \quad (40)$$

The leading-order bispectrum was derived in Refs. [22, 37] on the de Sitter background. In Ref. [22], the authors computed the three-point correlation function by taking into account all the possible slow-variation corrections to the leading-order term. In this case, the resulting bispectrum is valid for any shape of non-Gaussianities with the momentum triangle satisfying  $\mathbf{k}_1 + \mathbf{k}_2 + \mathbf{k}_3 = 0$ . Under the slow-variation approximation used above, the non-linear estimator  $f_{\text{NL}}^{\text{local}}$  in the squeezed limit ( $k_3 \rightarrow 0$ ,  $k_1 \rightarrow k_2$ ) is given by [22]

$$f_{\text{NL}}^{\text{local}} = \frac{5}{12} (1 - n_s). \quad (41)$$

Since  $f_{\text{NL}}^{\text{local}}$  is of the order of  $\epsilon$ , the Planck bound  $f_{\text{NL}}^{\text{local}} = 2.7 \pm 5.8$  (68 % CL) is satisfied for all the slow-variation single-field models based on the Horndeski's theories. There are some non slow-roll inflationary models in which the relation (41) can be violated [68], but we generally require the tunings of model parameters and initial conditions to satisfy the constraints of  $n_s$  and  $r$ . Hence we do not consider such specific models in our paper.

In Ref. [22], it was shown that the leading-order bispectrum (of the order of  $\epsilon^0$ ) can be expressed by the linear combination of two bases  $S_7^{\text{equil}}$  and  $S_7^{\text{ortho}}$ , as

$$\mathcal{A}_{\mathcal{R}}^{\text{lead}} = c_1 S_7^{\text{equil}} + c_2 S_7^{\text{ortho}}. \quad (42)$$

The coefficients  $c_1$  and  $c_2$  are

$$c_1 = \frac{13}{12} \left[ \frac{1}{24} \left( 1 - \frac{1}{c_s^2} \right) (2 + 3\beta) + \frac{\mu}{12\Sigma} (2 - 3\beta) - \frac{2 - 3\beta}{6} \frac{\delta_{G3X} + \delta_{G3XX} + 4(3\delta_{G4XX} + 2\delta_{G4XXX}) + \delta_{G5X} + 5\delta_{G5XX} + 2\delta_{G5XXX}}{\epsilon_s} + \frac{\delta_{G3X} + 6\delta_{G4XX} + \delta_{G5X} + \delta_{G5XX}}{3\epsilon_s c_s^2} \right], \quad (43)$$

$$c_2 = \frac{14 - 13\beta}{12} \left[ \frac{1}{8} \left( 1 - \frac{1}{c_s^2} \right) - \frac{\mu}{4\Sigma} + \frac{\delta_{G3X} + \delta_{G3XX} + 4(3\delta_{G4XX} + 2\delta_{G4XXX}) + \delta_{G5X} + 5\delta_{G5XX} + 2\delta_{G5XXX}}{2\epsilon_s} \right], \quad (44)$$

where  $\beta = 1.1967996 \dots$ , and

$$\begin{aligned} \mu = & \frac{F^2}{3} [3X^2 P_{,XX} + 2X^3 P_{,XXX} + 3H\dot{\phi}(XG_{3,X} + 5X^2 G_{3,XX} + 2X^3 G_{3,XXX}) - 2(2X^2 G_{3,\phi X} + X^3 G_{3,\phi XX}) \\ & + 6H^2(9X^2 G_{4,XX} + 16X^3 G_{4,XXX} + 4X^4 G_{4,XXXX}) - 3H\dot{\phi}(3X G_{4,\phi X} + 12X^2 G_{4,\phi XX} + 4X^3 G_{4,\phi XXX}) \\ & + H^3\dot{\phi}(3X G_{5,X} + 27X^2 G_{5,XX} + 24X^3 G_{5,XXX} + 4X^4 G_{5,XXXX}) \\ & - 6H^2(6X^2 G_{5,\phi X} + 9X^3 G_{5,\phi XX} + 2X^4 G_{5,\phi XXX})], \end{aligned} \quad (45)$$

$$\Sigma = \frac{w_1(4w_1w_3 + 9w_2^2)}{12M_{\text{pl}}^4}. \quad (46)$$

The shape functions  $S_7^{\text{equil}}$  and  $S_7^{\text{ortho}}$ , which have high correlations with the equilateral and orthogonal templates respectively, are given by

$$S_7^{\text{equil}} = -\frac{12}{13} \frac{1}{K} \left( 1 + \frac{1}{K^2} \sum_{i>j} k_i k_j + \frac{3k_1 k_2 k_3}{K^3} \right) \left[ \frac{3}{4} \sum_i k_i^4 - \frac{3}{2} \sum_{i>j} k_i^2 k_j^2 \right], \quad (47)$$

$$S_7^{\text{ortho}} = \frac{12}{14 - 13\beta} \left[ -\frac{13}{12} \beta S_7^{\text{equil}} + \frac{4}{K} \sum_{i>j} k_i^2 k_j^2 - \frac{2}{K^2} \sum_{i \neq j} k_i^2 k_j^3 - \frac{1}{2} \sum_i k_i^3 \right], \quad (48)$$

where  $K = k_1 + k_2 + k_3$ . These functions are normalized as  $S_7^{\text{equil}} = S_7^{\text{ortho}} = k^3$  at  $k_1 = k_2 = k_3 \equiv k$ . In the limit of the equilateral triangle ( $k_1 = k_2 = k_3$ ), the leading-order non-linear parameter  $f_{\text{NL}}^{\text{eq}} = 10\mathcal{A}_{\mathcal{R}}^{\text{lead}}/(9k^3)$  reads

$$\begin{aligned} f_{\text{NL}}^{\text{eq}} = & \frac{85}{324} \left( 1 - \frac{1}{c_s^2} \right) - \frac{10}{81} \frac{\mu}{\Sigma} + \frac{20}{81\epsilon_s} [\delta_{G3X} + \delta_{G3XX} + 4(3\delta_{G4XX} + 2\delta_{G4XXX}) + \delta_{G5X} + 5\delta_{G5XX} + 2\delta_{G5XXX}] \\ & + \frac{65}{162c_s^2\epsilon_s} (\delta_{G3X} + 6\delta_{G4XX} + \delta_{G5X} + \delta_{G5XX}). \end{aligned} \quad (49)$$

For the models in which  $c_s^2$  is of the order of 1,  $|f_{\text{NL}}^{\text{eq}}|$  is at most of the order of 1. However, the models with  $c_s^2 \ll 1$  (such as k-inflation) are subject to be constrained from the non-Gaussianities.

### III. CLASSIFICATION OF SINGLE-FIELD MODELS

In this section, we classify single-field inflationary models based on the Horndeski's theories and evaluate the inflationary observables in each model.

#### A. Potential-driven slow-roll inflation

The standard slow-roll inflation driven by a potential energy  $V(\phi)$  of a canonical field  $\phi$  is given by

$$P(\phi, X) = X - V(\phi), \quad G_3 = 0, \quad G_4 = 0, \quad G_5 = 0. \quad (50)$$

In this case,  $\epsilon = \epsilon_s = \delta_{PX} = \dot{\phi}^2/(2M_{\text{pl}}^2 H^2)$ ,  $c_s^2 = 1$ ,  $s = 0$ , and  $\delta_F = 0$ . Under the slow-roll approximation ( $\dot{\phi}^2/2 \ll V$ ), we have  $3M_{\text{pl}}^2 H^2 \simeq V$  from Eq. (4). Taking the time-derivative of this equation and using Eq. (5), it follows that  $\dot{\phi} \simeq -V_{,\phi}/(3H)$ . Then, the number of e-foldings (12) reads

$$N \simeq \frac{1}{M_{\text{pl}}^2} \int_{\phi_f}^{\phi} \frac{V}{V_{,\tilde{\phi}}} d\tilde{\phi}. \quad (51)$$

The slow-roll parameters  $\epsilon_s$  and  $\eta_s$  reduce to  $\epsilon_s \simeq \epsilon_V$  and  $\eta_s \simeq 4\epsilon_V - 2\eta_V$ , where

$$\epsilon_V \equiv \frac{M_{\text{pl}}^2}{2} \left( \frac{V_{,\phi}}{V} \right)^2, \quad \eta_V \equiv \frac{M_{\text{pl}}^2 V_{,\phi\phi}}{V}. \quad (52)$$

The observables (27), (34), and (35) reduce to

$$n_s = 1 - 6\epsilon_V + 2\eta_V, \quad r = -8n_t, \quad n_t = -2\epsilon_V. \quad (53)$$

Using Eqs. (51)-(53), we obtain the relation  $(d\phi/dN)^2 = (M_{\text{pl}}^2/8)r$ . Assuming that  $r$  is nearly constant, the variation  $\Delta\phi$  of the field during inflation (corresponding to  $N \approx 60$ ) can be estimated as

$$\Delta\phi/M_{\text{pl}} \approx \mathcal{O}(1) \times (r/0.01)^{1/2}. \quad (54)$$

This is known as the Lyth bound [69], which relates  $\Delta\phi$  with the tensor-to-scalar ratio  $r$ . The models with  $\Delta\phi \gtrsim M_{\text{pl}}$  and  $\Delta\phi \lesssim M_{\text{pl}}$  are called the “large-field” and “small-field” models, respectively.

Let us consider the power-law potential [4]

$$V(\phi) = \lambda\phi^n/n, \quad (55)$$

where  $n$  and  $\lambda$  are positive constants. In this case, we have  $\epsilon_V = n^2 M_{\text{pl}}^2/(2\phi^2)$  and  $\eta_V = n(n-1)M_{\text{pl}}^2/\phi^2$ . The field value  $\phi_f$  at the end of inflation can be derived from the condition  $\epsilon_V(\phi_f) = 1$ , that is,  $\phi_f = nM_{\text{pl}}/\sqrt{2}$ . From Eq. (51) the number of e-foldings  $N$  is related to the field  $\phi$ , as  $\phi^2(N) \simeq 2n(N + n/4)M_{\text{pl}}^2$ . Then, it follows that

$$n_s = 1 - \frac{2(n+2)}{4N+n}, \quad r = \frac{16n}{4N+n} = \frac{8n}{n+2}(1-n_s). \quad (56)$$

For the exponential potential  $V(\phi) = V_0 e^{-\gamma\phi/M_{\text{pl}}}$  [70, 71], we have  $n_s = 1 - \gamma^2$  and  $r = 8\gamma^2$ , so this model is on the line

$$r = 8(1-n_s), \quad (57)$$

which corresponds to the limit  $n \rightarrow \infty$  in the last relation of Eq. (56). Since inflation does not end for the exponential potential, we require the modification of the potential around the end of inflation.

## B. Non-minimally coupled models

We proceed to non-minimally coupled theories described by the action

$$S = \int d^4x \sqrt{-g} \left[ \frac{M_{\text{pl}}^2}{2} F(\phi) R + \omega(\phi) X - V(\phi) \right], \quad (58)$$

where  $F(\phi)$ ,  $\omega(\phi)$ , and  $V(\phi)$  are functions of  $\phi$ . From Eqs. (23)-(25) and (45)-(46), we have  $c_s^2 = 1$ ,  $s = 0$ , and  $\mu/\Sigma = 0$ .

Under the conformal transformation  $\hat{g}_{\mu\nu} = F(\phi)g_{\mu\nu}$ , the action (58) recasts to the one with a minimally coupled scalar field (the Einstein frame) [72]. The transformed action is given by

$$S_E = \int d^4x \sqrt{-\hat{g}} \left[ \frac{1}{2} M_{\text{pl}}^2 \hat{R} - \frac{1}{2} \hat{g}^{\mu\nu} \partial_\mu \chi \partial_\nu \chi - U(\chi) \right], \quad (59)$$

where a hat represents the quantities in the Einstein frame, and

$$U = \frac{V}{F^2}, \quad \chi \equiv \int B(\phi) d\phi, \quad B(\phi) \equiv \sqrt{\frac{3}{2} \left( \frac{M_{\text{pl}} F_{,\phi}}{F} \right)^2 + \frac{\omega}{F}}. \quad (60)$$

In Refs. [73–75], it was shown that inflationary observables such as  $n_s$  and  $r$  are unchanged even after the conformal transformation (i.e.,  $\hat{n}_s = n_s$  and  $\hat{r} = r$ ). Then, we just need to use the formulas (53) by replacing  $\epsilon_V$  and  $\eta_V$  for  $\epsilon_U = (M_{\text{pl}}^2/2)(U_{,\chi}/U)^2$  and  $\eta_U = M_{\text{pl}}^2 U_{,\chi\chi}/U$ , respectively.

Let us study the non-minimal coupling models given by [44–46]

$$F(\phi) = 1 - \xi\phi^2/M_{\text{pl}}^2, \quad (61)$$

with the non-canonical kinetic term  $\omega(\phi)X$ . For the self-coupling potential  $V(\phi) = \lambda\phi^4/4$ , the presence of the non-minimal coupling allows a possibility of reducing  $r$  [74, 75]. In particular, the Higgs potential  $V(\phi) = (\lambda/4)(\phi^2 - \phi_0^2)^2$



with  $\lambda \sim 0.1$  and  $\phi_0 \ll M_{\text{pl}}$  can be accommodated for largely negative values of  $\xi$  [46]. This comes from the fact that the amplitude of curvature perturbations is proportional to  $\lambda/\xi^2$  in the regime  $|\xi| \gg 1$ .

In the Einstein frame, the power-law potential (55) takes the form

$$U = \frac{\lambda \phi^n}{n(1 - \xi x^2)^2}, \quad \text{where} \quad x \equiv \frac{\phi}{M_{\text{pl}}}. \quad (62)$$

For  $n = 4$  and  $\xi < 0$ , this potential is asymptotically flat in the regime  $\phi \gg M_{\text{pl}}$ . From Eq. (53), the scalar spectral index and the tensor-to-scalar ratio for the potential (62) read [48]

$$n_s - 1 = -\frac{1}{[\omega + (6\xi - \omega)\xi x^2]^2 x^2} \left\{ (n-4)^2(6\xi - \omega)(\xi x^2)^3 + (24\omega - 14n\omega + 3n^2\omega + 24n\xi - 12n^2\xi)(\xi x^2)^2 \right. \\ \left. + (-8\omega + 4n\omega - 3n^2\omega + 24n\xi + 6n^2\xi)\xi x^2 + n\omega(n+2) - \mu\omega x(1 - \xi x^2)^2[(n-4)\xi x^2 - n] \right\}, \quad (63)$$

$$r = -8n_t = \frac{8[n + (4-n)\xi x^2]^2}{x^2[\omega + (6\xi - \omega)\xi x^2]}, \quad (64)$$

where  $\mu \equiv M_{\text{pl}}\omega_{,\phi}/\omega$ . The scalar power spectrum (26) is given by

$$\mathcal{P}_{\mathcal{R}} = \frac{U^3}{12\pi^2 M_{\text{pl}}^6 U_{,\chi}^2} = \frac{\lambda M_{\text{pl}}^{n-4}}{12\pi^2 n} \frac{x^{n+2}[6\xi^2 x^2 + \omega(1 - \xi x^2)]}{(1 - \xi x^2)^2[n + (4-n)\xi x^2]^2}. \quad (65)$$

For the models with constant  $\omega$ , we have  $\mu = 0$ .

The Hubble parameters in the Jordan and Einstein frames ( $H$  and  $\hat{H}$  respectively) have the relation  $\hat{H} = [H + \dot{F}/(2F)]/\sqrt{F}$ . The number of e-foldings in the Einstein frame should be the same as that in the Jordan frame by properly choosing a reference length scale [76]. Under the slow-roll approximation, the frame-independent quantity (12) reads [48]

$$N = \int_{\chi_f}^{\chi} \frac{U}{M_{\text{pl}}^2 U_{,\chi}} d\chi + \frac{1}{2} \ln \frac{F}{F_f}, \quad (66)$$

where the subscript “ $f$ ” represents the value at the end of inflation (which is determined by the condition  $\epsilon_U = 1$ ). For the potential (62) it follows that

$$N = -\frac{1}{4\xi} \ln \left| \frac{(n-4)\xi x_f^2 - n}{(n-4)\xi x^2 - n} \right|^{\frac{3n\xi - 2\omega}{n-4}} - \frac{1}{4} \ln \left| \frac{1 - \xi x^2}{1 - \xi x_f^2} \right| \quad (n \neq 4), \quad (67)$$

$$N = \frac{\omega - 6\xi}{8} (x^2 - x_f^2) - \frac{1}{4} \ln \left| \frac{1 - \xi x^2}{1 - \xi x_f^2} \right| \quad (n = 4), \quad (68)$$

where

$$x_f^2 = \frac{\omega - \xi n(4-n) - \sqrt{(\omega - 2n\xi)(\omega - 6n\xi)}}{\xi[\xi(4-n)^2 + 2(\omega - 6\xi)]}. \quad (69)$$

### C. Running kinetic couplings

Running kinetic inflation is characterized by the action (58) in the presence of the field-dependent coupling  $\omega(\phi)$  with  $F(\phi) = 1$ . We focus on the case of the exponential coupling [48]

$$\omega(\phi) = e^{\mu\phi/M_{\text{pl}}}, \quad (70)$$

where  $\mu$  is constant. This is motivated by the dilatonic coupling in low-energy effective string theory [77]. For concreteness, we take the power-law potential (55). At the potential minimum ( $\phi = 0$ ), the coupling  $\omega(\phi)$  is equivalent to 1.



The spectral index (63) and the tensor-to-scalar ratio (64) read

$$n_s - 1 = -\frac{n}{x^2 e^{\mu x}}(n + 2 + \mu x), \quad r = -8n_t = \frac{8n^2}{x^2 e^{\mu x}}, \quad (71)$$

where  $x = \phi/M_{\text{pl}}$ . From Eq. (66), the number of e-foldings is

$$N = \frac{1}{n\mu^2} [(\mu x - 1)e^{\mu x} - (\mu x_f - 1)e^{\mu x_f}], \quad (72)$$

where the field value at the end of inflation is known by solving  $x_f^2 e^{\mu x_f} = n^2/2$ .

#### D. Brans-Dicke theories (including $f(R)$ gravity)

The Brans-Dicke (BD) theory is described by the action

$$S = \int d^4x \sqrt{-g} \left[ \frac{1}{2} M_{\text{pl}} \phi R + \frac{M_{\text{pl}}}{\phi} \omega_{\text{BD}} X - V(\phi) \right], \quad (73)$$

where  $\omega_{\text{BD}}$  is the BD parameter. Contrary to the original BD theory [49], we introduced the field potential  $V(\phi)$ . Since this theory belongs to a class of the action (58), the action in the Einstein frame is given by Eq. (59) with

$$U = e^{-2\gamma\chi/M_{\text{pl}}} V, \quad F = \phi/M_{\text{pl}} = e^{\gamma\chi/M_{\text{pl}}}, \quad \gamma = 1/\sqrt{3/2 + \omega_{\text{BD}}}. \quad (74)$$

The scalar and tensor ghosts are absent under the conditions  $\omega_{\text{BD}} > -3/2$  and  $F > 0$ .

The  $f(R)$  theory characterized by the action  $S = \int d^4x \sqrt{-g} M_{\text{pl}}^2 f(R)/2$  is a subclass of the BD theory (73) with the correspondence

$$\frac{\phi}{M_{\text{pl}}} = \frac{\partial f}{\partial R}, \quad V(\phi) = \frac{M_{\text{pl}}^2}{2} \left( R \frac{\partial f}{\partial R} - f \right), \quad \omega_{\text{BD}} = 0. \quad (75)$$

The Starobinsky's model of inflation [1] corresponds to the Lagrangian

$$f(R) = R + \frac{R^2}{6M^2}, \quad (76)$$

where  $M$  is a constant having a dimension of mass. In this case, the potential  $V(\phi)$  in the Jordan frame reads

$$V(\phi) = \frac{3M^2}{4} (\phi - M_{\text{pl}})^2, \quad (77)$$

where  $\phi/M_{\text{pl}} = 1 + R/(3M^2)$ .

We study the BD theory described by the action (73) with the field potential (77). This analysis covers the  $f(R)$  model (76) as a special case ( $\omega_{\text{BD}} = 0$ ). The potential in the Einstein frame reads

$$U(\chi) = \frac{3}{4} M^2 M_{\text{pl}}^2 \left( 1 - e^{-\gamma\chi/M_{\text{pl}}} \right)^2. \quad (78)$$

Inflation occurs in the regime  $\gamma\chi/M_{\text{pl}} \gg 1$ , which is followed by the reheating stage characterized by the potential  $U(\chi) \simeq (3/4)\gamma^2 M^2 \chi^2$ . For the potential (78), the inflationary observables are [48]

$$n_s - 1 = -\frac{4\gamma^2(F+1)}{(F-1)^2}, \quad r = -8n_t = \frac{32\gamma^2}{(F-1)^2}. \quad (79)$$

The number of e-foldings (66) yields

$$N = \frac{1}{2\gamma^2} (F - F_f) + \frac{1}{2} \left( 1 - \frac{1}{\gamma^2} \right) \ln \left( \frac{F}{F_f} \right), \quad (80)$$

where  $F_f = 1 + \sqrt{2}\gamma$ .

### E. Potential-driven Galileon inflation

The potential-driven inflation with covariant Galileon terms [52, 78, 79] belongs to a class of the action (1) with the choice

$$P = X - V(\phi), \quad G_3 = \frac{c_3}{M^3}X, \quad G_4 = -\frac{c_4}{M^6}X^2, \quad G_5 = \frac{3c_5}{M^9}X^2. \quad (81)$$

From Eq. (10), we have

$$\epsilon = (1 + \mathcal{A})\delta_{PX}, \quad \text{where} \quad \mathcal{A} \equiv \frac{3\delta_{G3X} + 18\delta_{G4X} + 5\delta_{G5X}}{\delta_{PX}}. \quad (82)$$

Since inflation is mainly driven by the potential energy, Eq. (4) is approximately given by

$$3M_{\text{pl}}^2 H^2 \simeq V. \quad (83)$$

Taking the time derivative of Eq. (83) and using Eq. (82), it follows that

$$3H\dot{\phi}(1 + \mathcal{A}) \simeq -V_{,\phi}. \quad (84)$$

From Eqs. (83) and (84), we have  $\delta_{PX} \simeq \epsilon_V/(1 + \mathcal{A})^2$  and hence  $\epsilon \simeq \epsilon_V/(1 + \mathcal{A})$ . The field value at the end of inflation is known by  $\epsilon(\phi_f) = 1$ , i.e.,

$$\epsilon_V(\phi_f) = 1 + \mathcal{A}(\phi_f). \quad (85)$$

Using Eqs. (83) and (84), the number of e-foldings (12) reads

$$N \simeq \frac{1}{M_{\text{pl}}^2} \int_{\phi_f}^{\phi} (1 + \mathcal{A}) \frac{V}{V_{,\tilde{\phi}}} d\tilde{\phi}. \quad (86)$$

In the regime  $\mathcal{A} \gg 1$ , the Galileon self-interaction dominates over the standard kinetic term  $X$ .

The quantities  $q_s$  and  $c_s^2$  in Eqs. (23) and (25) reduce to

$$q_s = \delta_{PX} + 6\delta_{G3X} + 54\delta_{G4X} + 20\delta_{G5X}, \quad (87)$$

$$c_s^2 = \frac{\delta_{PX} + 4\delta_{G3X} + 26\delta_{G4X} + 8\delta_{G5X}}{\delta_{PX} + 6\delta_{G3X} + 54\delta_{G4X} + 20\delta_{G5X}}. \quad (88)$$

In order to avoid the appearance of scalar ghosts and Laplacian instabilities in the regime  $\mathcal{A} \gg 1$ , we demand the conditions  $c_3\dot{\phi} > 0$ ,  $c_4 < 0$ , and  $c_5\dot{\phi} > 0$ . In the case where either of  $\delta_{G3X}$ ,  $\delta_{G4X}$ ,  $\delta_{G5X}$  dominates over  $\delta_{PX}$  during inflation, the scalar propagation speed squared is  $c_s^2 = 2/3, 13/27, 2/5$ , respectively. This leads to the modification of the consistency relation  $r = -8n_t$  in standard potential-driven slow-roll inflation. Using Eqs. (24), (82), and (88), the tensor-to-scalar ratio (34) and the tensor spectral index (35) reduce to

$$r = 16 \frac{(\delta_{PX} + 4\delta_{G3X} + 26\delta_{G4X} + 8\delta_{G5X})^{3/2}}{(\delta_{PX} + 6\delta_{G3X} + 54\delta_{G4X} + 20\delta_{G5X})^{1/2}}, \quad (89)$$

$$n_t = -2(\delta_{PX} + 3\delta_{G3X} + 18\delta_{G4X} + 5\delta_{G5X}). \quad (90)$$

If either of  $\delta_{G3X}$ ,  $\delta_{G4X}$ ,  $\delta_{G5X}$  dominates over  $\delta_{PX}$  during inflation, the relation between  $r$  and  $n_t$  is

$$r = -8.709 n_t, \quad (G_3 \text{ dominant}), \quad (91)$$

$$r = -8.018 n_t, \quad (G_4 \text{ dominant}), \quad (92)$$

$$r = -8.095 n_t, \quad (G_5 \text{ dominant}). \quad (93)$$

For the Galileon model in which only one of the  $G_i$  terms ( $i = 3, 4, 5$ ) is present, Eqs. (26), (27), and (34) can be written in the forms [79]

$$\mathcal{P}_{\mathcal{R}} = \frac{V^3}{12\pi^2 M_{\text{pl}}^6 V_{,\phi}^2} f_i(\mathcal{A}), \quad n_s - 1 = -6\epsilon_V g_{\epsilon i}(\mathcal{A}) + 2\eta_V g_{\eta i}(\mathcal{A}), \quad r = 16\epsilon_V h_i(\mathcal{A}), \quad (94)$$

where the functions  $f_i$ ,  $g_{\epsilon i}$ ,  $g_{\eta i}$ , and  $h_i$  are

$$f_3(\mathcal{A}) = \frac{(1+\mathcal{A})^2(1+2\mathcal{A})^{1/2}}{(1+4\mathcal{A}/3)^{3/2}}, \quad f_4(\mathcal{A}) = \frac{(1+\mathcal{A})^2(1+3\mathcal{A})^{1/2}}{(1+13\mathcal{A}/9)^{3/2}}, \quad f_5(\mathcal{A}) = \frac{(1+\mathcal{A})^2(1+4\mathcal{A})^{1/2}}{(1+8\mathcal{A}/5)^{3/2}}, \quad (95)$$

$$g_{\epsilon 3}(\mathcal{A}) = g_{\epsilon 4}(\mathcal{A}) = g_{\epsilon 5}(\mathcal{A}) = \frac{1}{1+\mathcal{A}}, \quad (96)$$

$$g_{\eta 3}(\mathcal{A}) = \frac{6+23\mathcal{A}+24\mathcal{A}^2}{2(1+2\mathcal{A})^2(3+4\mathcal{A})}, \quad g_{\eta 4}(\mathcal{A}) = \frac{9+46\mathcal{A}+78\mathcal{A}^2}{(1+3\mathcal{A})^2(9+13\mathcal{A})}, \quad g_{\eta 5}(\mathcal{A}) = \frac{5+31\mathcal{A}+80\mathcal{A}^2}{(1+4\mathcal{A})^2(5+8\mathcal{A})}, \quad (97)$$

$$h_3(\mathcal{A}) = \frac{(1+4\mathcal{A}/3)^{3/2}}{(1+\mathcal{A})^2(1+2\mathcal{A})^{1/2}}, \quad h_4(\mathcal{A}) = \frac{(1+13\mathcal{A}/9)^{3/2}}{(1+\mathcal{A})^2(1+3\mathcal{A})^{1/2}}, \quad h_5(\mathcal{A}) = \frac{(1+8\mathcal{A}/5)^{3/2}}{(1+\mathcal{A})^2(1+4\mathcal{A})^{1/2}}. \quad (98)$$

The amplitude  $\mathcal{P}_{\mathcal{R}}$  is constrained to be  $\mathcal{P}_{\mathcal{R}} \simeq 2.2 \times 10^{-9}$  at  $k_0 = 0.002 \text{ Mpc}^{-1}$  from the Planck data [13]. For the power-law potential (55), this provides a relation between  $\lambda$  and  $M$  for a given value of  $n$ .

### F. Field-derivative couplings to the Einstein tensor

The model of the field-derivative couplings to the Einstein tensor is given by the action [53, 54]

$$\mathcal{S} = \int d^4x \sqrt{-g} \left[ \frac{M_{\text{pl}}^2}{2} R + X - V(\phi) + \frac{1}{2M^2} G^{\mu\nu} \partial_\mu \phi \partial_\nu \phi \right], \quad (99)$$

where  $M$  is a constant having a dimension of mass. In the Horndeski's action, this corresponds to the choice  $G_5(\phi) = -\phi/(2M^2)$  (with integration by parts) [50, 80].

From Eqs. (10) and (4), the same equations as Eqs. (82), (83), and (84) hold with the replacement

$$\mathcal{A} \equiv -\frac{6\delta_{G_5\phi}}{\delta_{PX}} = \frac{3H^2}{M^2} \simeq \frac{V}{M^2 M_{\text{pl}}^2}. \quad (100)$$

There is also the relation  $\epsilon = \epsilon_V/(1+\mathcal{A})$ . The field value  $\phi_f$  at the end of inflation and the number of e-foldings  $N$  are known from Eqs. (85) and (86), respectively.

Since  $q_s = \delta_{PX} - 6\delta_{G_5\phi}$ , the condition  $q_s > 0$  is automatically satisfied for  $G_5 = -\phi/(2M^2)$ . We also have  $c_s^2 = 1$  at leading order of slow-roll. Since  $\epsilon_s = \epsilon = \delta_{PX} - 6\delta_{G_5\phi}$ , the consistency relation is [81]

$$r = -8n_t, \quad (101)$$

which is the same as that of standard slow-roll inflation. Equations (26), (27), and (34) can be expressed as [80]

$$\mathcal{P}_{\mathcal{R}} = \frac{V^3}{12\pi^2 M_{\text{pl}}^6 V_{,\phi}^2} (1+\mathcal{A}), \quad n_s - 1 = -6\epsilon_V \frac{1+4\mathcal{A}/3}{(1+\mathcal{A})^2} + 2\eta_V \frac{1}{1+\mathcal{A}}, \quad r = \frac{16\epsilon_V}{1+\mathcal{A}}. \quad (102)$$

For the power-law potential (55),  $n_s$  and  $r$  reduce to

$$n_s = 1 - \frac{n^2[n(n+2) + 2(n+1)\alpha x^n]}{x^2(n + \alpha x^n)^2}, \quad r = \frac{8n^3}{x^2(n + \alpha x^n)}, \quad (103)$$

where  $\alpha = \lambda M_{\text{pl}}^{n-2}/M^2$  and  $x = \phi/M_{\text{pl}}$ . The number of e-foldings is given by

$$N = \frac{x^2}{2n} \left[ 1 + \frac{2\alpha}{n(n+2)} x^n \right] - \frac{x_f^2}{2n} \left[ 1 + \frac{2\alpha}{n(n+2)} x_f^n \right], \quad (104)$$

where  $x_f$  is known by solving  $2x_f^2(1 + \alpha x_f^n/n) = n^2$ .

### G. k-inflation

We consider the k-inflationary scenario in which the non-linear terms of  $X$  are present in the Lagrangian [25]. In the following, we focus on the models in which the scalar propagation speed  $c_s$  is constant. In fact, the constant values

of  $c_s$  appear in the context of power-law k-inflation ( $a \propto t^p$  with constant  $p$ ). Generally, such a power-law expansion can be realized for the Lagrangian [65]

$$P(\phi, X) = X g(Y), \quad Y \equiv X e^{\lambda \phi}, \quad (105)$$

where  $g$  is an arbitrary function of  $Y$ , and  $\lambda$  is a constant. Originally, the Lagrangian (105) was derived for the existence of scaling solutions in the presence of a barotropic fluid [62, 82]. Under the condition  $\lambda^2 < 2P_{,X}$ , there exists a power-law inflationary solution [83]. In the presence of multiple scalar fields with the Lagrangian  $P = \sum_{i=1}^n X_i g(X_i e^{\lambda_i \phi_i})$ , assisted inflation can be realized with the effective slope  $\lambda = (\sum_{i=1}^n 1/\lambda_i^2)^{-1/2}$ . The simplest example is a canonical field with an exponential potential ( $g(Y) = 1 - c/Y$ , i.e.,  $P = X - c e^{-\lambda \phi}$ ) [71]. Thus, the Lagrangian (105) not only realizes power-law inflation with constant  $c_s$ , but also it corresponds to the effective single-field Lagrangian of assisted inflation.

For the Lagrangian (105), the background equations (4) and (5) read

$$3M_{\text{pl}}^2 H^2 = X(g + 2g_1), \quad \epsilon = \frac{3(g + g_1)}{g + 2g_1}, \quad (106)$$

where  $g_n \equiv Y^n (d^n g / dY^n)$ . If we define the field equation of state as  $w_\phi = P / (2X P_{,X} - P)$ , the power-law inflationary solution mentioned above corresponds to  $w_\phi = -1 + \lambda^2 / (3P_{,X})$  [65, 83]. Then, this solution satisfies the relation  $\lambda = 6(g + g_1)^2 / (g + 2g_1)$ , along which  $Y$  and  $\epsilon$  are constants. From Eqs. (27), (34), and (35), we have

$$n_s - 1 = -2\epsilon = n_t, \quad (107)$$

$$r = 16c_s \epsilon = -8c_s n_t, \quad (108)$$

where the scalar propagation speed squared is

$$c_s^2 = \frac{g + g_1}{g + 5g_1 + 2g_2}, \quad (109)$$

which is constant along the power-law inflationary solution. The leading-order non-linear estimator (49) of the equilateral triangle ( $k_1 = k_2 = k_3$ ) reads

$$f_{\text{NL}}^{\text{eq}} = \frac{85}{324} \left( 1 - \frac{1}{c_s^2} \right) - \frac{10}{243} \frac{6g_1 + 9g_2 + 2g_3}{g + 5g_1 + 2g_2}. \quad (110)$$

For a given model (i.e., for a given form of  $g(Y)$ ), the variable  $Y$  is known in terms of  $c_s$ . Then, the quantities (107), (108), and (110) can be expressed with respect to  $c_s$ . Note that, in order to exit from the regime of power-law k-inflation, the Lagrangian needs to be modified around the end of inflation. We assume that for the scales relevant to the CMB anisotropies the Lagrangian is well approximated by Eq. (105). In the following, we consider two representative models of k-inflation.

### 1. Dilatonic ghost condensate

The dilatonic ghost condensate model [62], which is a generalization of the ghost condensate model [84], is described by the Lagrangian

$$P = -X + c e^{\lambda \phi} X^2, \quad (111)$$

where  $c$  is a constant. By making a field redefinition [82], one can show that this is equivalent to the model  $P \propto \phi^{-2}(-X + X^2/M^4)$  first discussed in Ref. [25]. The Lagrangian (111) corresponds to the function  $g(Y) = -1 + cY$  in Eq. (105). Since  $\epsilon = 3(2cY - 1)/(3cY - 1)$ ,  $c_s^2 = (2cY - 1)/(6cY - 1)$ , and  $\mu/\Sigma = (1 - c_s^2)/2$  in this case, it follows that

$$n_s - 1 = n_t = -\frac{24c_s^2}{1 + 3c_s^2}, \quad r = \frac{192c_s^3}{1 + 3c_s^2}, \quad f_{\text{NL}}^{\text{eq}} = -\frac{85}{324} \frac{1}{c_s^2} + \frac{5}{81} c_s^2 + \frac{65}{324}, \quad (112)$$

which are written in terms of  $c_s$  alone.

## 2. DBI model

The DBI model [63] is given by the Lagrangian

$$P = -f^{-1}(\phi)\sqrt{1 - 2f(\phi)\dot{X}} + f^{-1}(\phi) - V(\phi), \quad (113)$$

where  $f(\phi)$  and  $V(\phi)$  are functions of  $\phi$ . If we choose the function  $g(Y) = -(m^4/Y)\sqrt{1 - 2Y/m^4} - M^4/Y$  with two constant mass scales  $m$  and  $M$ , we obtain the Lagrangian (113) with

$$f^{-1}(\phi) = m^4 e^{-\lambda\phi}, \quad V(\phi) = m^4(c_M + 1)e^{-\lambda\phi}, \quad \text{where } c_M \equiv M^4/m^4. \quad (114)$$

In this case, we have

$$\epsilon = \frac{3\tilde{Y}}{1 + c_M\sqrt{1 - 2\tilde{Y}}}, \quad c_s^2 = 1 - 2\tilde{Y}, \quad \text{where } \tilde{Y} \equiv Y/m^4. \quad (115)$$

Using the relation  $\mu/\Sigma = (1 - c_s^2)/(2c_s^2)$ , we obtain

$$n_s - 1 = n_t = -\frac{3(1 - c_s^2)}{1 + c_M c_s}, \quad r = \frac{24c_s(1 - c_s^2)}{1 + c_M c_s} = 8c_s(1 - n_s), \quad f_{\text{NL}}^{\text{eq}} = -\frac{35}{108} \left( \frac{1}{c_s^2} - 1 \right). \quad (116)$$

The ultra-relativistic regime ( $c_s \ll 1$ ) corresponds to the case where  $\tilde{Y}$  is close to  $1/2$ . If  $c_M$  is much larger than 1, the condition  $c_M c_s \gg 1$  can be satisfied even for  $c_s \ll 1$ . In this case, both  $n_s - 1$  and  $r$  are much smaller than 1. When  $c_s \ll 1$ ,  $|f_{\text{NL}}^{\text{eq}}|$  can be much larger than 1.

## IV. JOINT OBSERVATIONAL CONSTRAINTS ON SINGLE-FIELD INFLATIONARY MODELS

In this section, we put observational constraints on each inflationary model discussed in the previous section. In doing so, we expand the power spectra  $\mathcal{P}_{\mathcal{R}}$  and  $\mathcal{P}_h$  around the pivot wave number  $k_0$ , as

$$\ln \mathcal{P}_{\mathcal{R}}(k) = \ln \mathcal{P}_{\mathcal{R}}(k_0) + [n_s(k_0) - 1]y + \frac{\alpha_s(k_0)}{2}y^2 + \mathcal{O}(y^3), \quad (117)$$

$$\ln \mathcal{P}_h(k) = \ln \mathcal{P}_h(k_0) + n_t(k_0)y + \frac{\alpha_t(k_0)}{2}y^2 + \mathcal{O}(y^3), \quad (118)$$

where  $y = \ln(k/k_0)$ . For the validity of the Taylor expansion, we require the following conditions

$$|\alpha_s(k_0)| < 2|[n_s(k_0) - 1]/y|, \quad |\alpha_t(k_0)| < 2|n_t(k_0)/y|. \quad (119)$$

Under the slow-variation approximation, both  $|\alpha_s(k_0)|$  and  $|\alpha_t(k_0)|$  are of the order of  $\epsilon^2$ , whereas  $|n_s(k_0) - 1|$  and  $|n_t(k_0)|$  are  $\mathcal{O}(\epsilon)$ . The value  $y$  depends on the choice of  $k_0$ . For the scales relevant to the CMB anisotropies ( $2 \leq l \lesssim 2500$ ),  $y$  is smaller than 7. Then, the convergence criteria (119) are well satisfied.

Following the Planck paper [13], we set both  $\alpha_s(k_0)$  and  $\alpha_t(k_0)$  to be 0 in the CMB likelihood analysis. This is valid for the slow-variation inflationary models. Then, we are left with four parameters  $\mathcal{P}_{\mathcal{R}}(k_0)$ ,  $n_s(k_0)$ ,  $r(k_0)$ , and  $n_t(k_0)$ . If we specify the models, there are some relations between  $n_s(k_0)$ ,  $r(k_0)$ , and  $n_t(k_0)$ . This allows us to reduce the number of free parameters.

We take the pivot wave number to be

$$k_0 = 0.05 \text{ Mpc}^{-1}, \quad (120)$$

which corresponds to a smaller scale relative to the value  $k_0 = 0.002 \text{ Mpc}^{-1}$  chosen by the Planck team. Around the pivot scale (120) the CMB spectrum is hardly affected by the uncertainty of cosmic variance. Note that we also performed the CosmoMC analysis for  $k_0 = 0.002 \text{ Mpc}^{-1}$  and reproduced the results presented in Ref. [13]. We confirmed that the likelihood results are insensitive to the choice of different values of  $k_0$ . We carry out the joint data analysis of Planck [11], WP [12], BAO [57–59], and high- $\ell$  [60, 61]. In comparison, we also show the likelihood contours constrained by the Planck+WP+BAO data.

In the whole analysis, the flat  $\Lambda$ CDM model is assumed with  $N_{\text{eff}} = 3.046$  relativistic degrees of freedom [85]. We employ the big bang nucleosynthesis consistency relation in that the helium fraction  $Y_p$  is expressed in terms of  $N_{\text{eff}}$  and the baryon fraction  $\Omega_b h^2$  [86]. We also assume that reionization occurs instantly at a redshift  $z_{\text{re}}$ .

In the following, we proceed to observational constraints on each inflationary model. For the scales relevant to the CMB anisotropies, we fix the number of e-foldings to be  $N = 60$ . In principle, we can choose smaller values of  $N$  like 50, but if some model is under an observational pressure for  $N = 60$ , it is typically more difficult to be compatible with observational constraints for  $N = 50$ . However, there are some exceptions, so we discuss such cases separately.

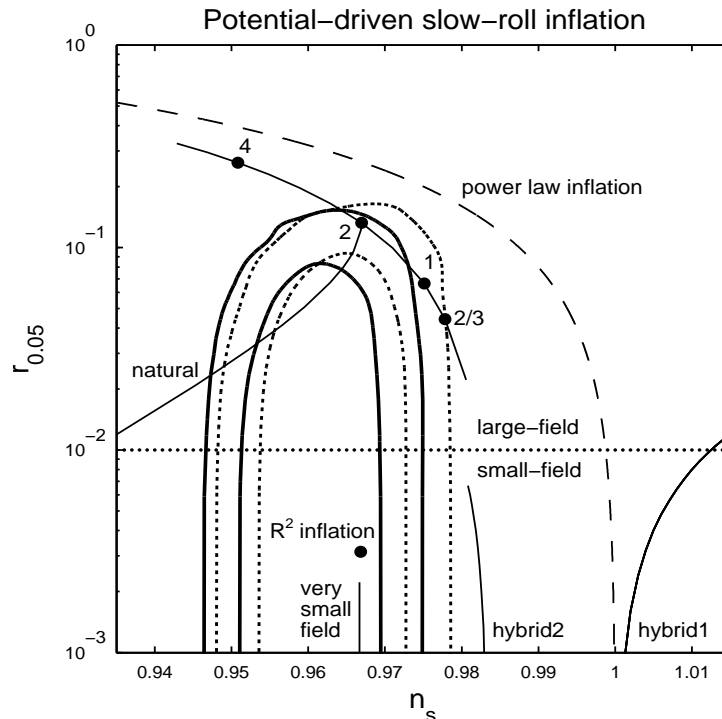


Figure 1: 2-dimensional observational constraints on potential-driven slow-roll inflation in the  $(n_s, r)$  plane with the number of e-foldings  $N = 60$  and the pivot wave number  $k_0 = 0.05 \text{ Mpc}^{-1}$ . The bold solid curves represent the 68 % CL (inside) and 95 % CL (outside) boundaries derived by the joint data analysis of Planck+WP+BAO+high- $\ell$ , whereas the dotted curves correspond to the 68 % and 95 % contours constrained by Planck+WP+BAO. In both cases the consistency relation  $r(k_0) = -8n_t(k_0)$  is used. We show the theoretical predictions for the models: (i) chaotic inflation with the potential  $V(\phi) = \lambda\phi^n/n$  for general  $n$  (thin solid curve) and for  $n = 4, 2, 1, 2/3$  (denoted as black circles), (ii) natural inflation with the potential  $V(\phi) = \Lambda^4[1 + \cos(\phi/f)]$  for general  $f$ , (iii) hybrid inflation with the potentials  $V(\phi) = \Lambda^4 + m^2\phi^2/2$  (“hybrid1”) and  $V(\phi) = \Lambda^4[1 + c\ln(\phi/\mu)]$  (“hybrid2”), (iv) very small-field inflation with the potential  $V(\phi) = \Lambda^4(1 - e^{-\phi/M})$  in the regime  $M < M_{\text{pl}}$ , and (v) power-law inflation with the exponential potential  $V(\phi) = V_0 e^{-\gamma\phi/M_{\text{pl}}}$ . The dotted line ( $r = 10^{-2}$ ) corresponds to the boundary between “large-field” and “small-field” models. For comparison, we also show the theoretical prediction of the Starobinsky’s model  $f(R) = R + R^2/(6M^2)$  (denoted as “ $R^2$  inflation”).

### A. Potential-driven slow-roll inflation

For the potential-driven slow-roll inflation with the Lagrangian (50), the consistency relation between  $r(k_0)$  and  $n_t(k_0)$  is given by  $r(k_0) = -8n_t(k_0)$ . With the CosmoMC code, we perform the likelihood analysis by varying the three inflationary parameters  $\mathcal{P}_{\mathcal{R}}(k_0)$ ,  $n_s(k_0)$  and  $r(k_0)$  together with other cosmological parameters.

The thick dotted curves in Fig. 1 correspond to the 68 % and 95 % CL boundaries in the  $(n_s, r)$  plane constrained by the joint data analysis of Planck, WP, and BAO. These bounds are similar to those derived by the Planck mission, in spite of the different choice of  $k_0$  (see Fig. 1 in Ref. [13]). The thick solid curves represent the 68 % and 95 % CL borders derived by the joint data analysis of the Planck, WP, BAO, and high- $\ell$  data. Adding the high- $\ell$  data leads to the shift of  $n_s$  toward smaller values and the slight decrease of  $r$ . While the Planck group showed the bounds obtained from the Planck, WP, and high- $\ell$  data in Fig. 1 of Ref. [13], we also included the BAO data. The latter gives tighter bounds on  $n_s$  than those constrained by the former. In the following, we place observational constraints on each inflaton potential.

#### 1. Chaotic inflation

For the power-law potential (55),  $n_s$  and  $r$  are given by Eq. (56). The quartic potential ( $n = 4$ ) gives the values  $n_s = 0.951$  and  $r = 0.262$  for  $N = 60$ , which is outside the 95 % CL contour. For the quadratic potential ( $n = 2$ ) with  $N = 60$ , we have  $n_s = 0.967$  and  $r = 0.132$ . This is close to the 95 % CL boundary constrained by the

Planck+WP+BAO+high- $\ell$  data.

The axion monodromy scenario [87] gives rise to the linear potential with  $n = 1$ . For  $N = 60$ , this potential is within the 95 % CL region constrained by the Planck+WP+BAO data, but it is outside the 95 % CL boundary by adding the high- $\ell$  data. This latter bound is tighter than that derived by the Planck team based on the Planck, WP, and high- $\ell$  data. For  $N = 50$ , however, we have  $n_s = 0.970$  and  $r = 7.96 \times 10^{-2}$ , so that the linear potential enters the joint 95 % CL region constrained by Planck+WP+BAO+high- $\ell$ . There is another power-law potential with  $n = 2/3$  appearing in axion monodromy [88]. For  $N = 60$ , this potential is outside the joint 95 % CL boundary constrained by Planck+WP+BAO+high- $\ell$ . For  $N = 50$ , we have  $n_s = 0.973$  and  $r = 5.32 \times 10^{-2}$ , in which case the model marginally lies within the 95 % CL contour.

The exponential potential  $V(\phi) = V_0 e^{-\gamma\phi/M_{\text{pl}}}$ , which gives rise to the power-law inflation  $a \propto t^{2/\gamma^2}$ , is characterized by the line (57) in the  $(n_s, r)$  plane. From Fig. 1, we find that this model (denoted as a dashed curve) is excluded at more than 95 % CL.

## 2. Natural inflation

Natural inflation is characterized by the potential

$$V(\phi) = \Lambda^4 [1 + \cos(\phi/f)] , \quad (121)$$

where  $\Lambda$  and  $f$  are constants having a dimension of mass. If inflation occurs in the region around  $\phi = 0$ , the expansion of Eq. (121) gives rise to the hill-top potential of the form  $V(\phi) = 2\Lambda^4 [1 - \phi^2/(4f^2) + \dots]$ . For the potential (121), the number of e-foldings is related to the field  $\phi$ , as  $N = (2f^2/M_{\text{pl}}^2) \ln[\sin(\phi_f/(2f))/\sin(\phi/(2f))]$ , where  $\phi_f$  is known by solving  $\tan^2[\phi_f/(2f)] = 2(f/M_{\text{pl}})^2$ . The inflationary observables are

$$n_s = 1 - \frac{M_{\text{pl}}^2}{f^2} \frac{3 - \cos(\phi/f)}{1 + \cos(\phi/f)} , \quad r = \frac{8M_{\text{pl}}^2}{f^2} \frac{\sin^2(\phi/f)}{[1 + \cos(\phi/f)]^2} . \quad (122)$$

For a given value of  $f$ , we can numerically identify the value of  $\phi$  at  $N = 60$ . Then,  $n_s$  and  $r$  are evaluated from Eq. (122). In the limit that  $f \rightarrow \infty$ , inflation occurs in the regime where  $\phi$  is close to the potential minimum ( $\phi = \pi f$ ). In this limit,  $n_s$  and  $r$  approach the values of chaotic inflation with  $n = 2$ , i.e.,  $n_s = 1 - 4/(2N + 1)$  and  $r = 16/(2N + 1)$ . For smaller  $f$ , both  $n_s$  and  $r$  tend to decrease.

In Fig. 1, we show the theoretical values of  $n_s$  and  $r$  for different values of  $f$ . There are intermediate values of  $f$  with which the model is within the 68 % CL region. From the joint data analysis of Planck+WP+BAO+high- $\ell$ , we obtain the following bounds

$$5.1M_{\text{pl}} < f < 7.9M_{\text{pl}} \quad (68 \text{ \% CL}) , \quad (123)$$

$$f > 4.6M_{\text{pl}} \quad (95 \text{ \% CL}) . \quad (124)$$

The bound (124) is tighter than  $f > 3.5M_{\text{pl}}$  derived in Ref. [89] with the WMAP data.

## 3. Hybrid inflation

Hybrid inflation is characterized by the potential

$$V(\phi) = \Lambda^4 + U(\phi) , \quad (125)$$

where  $\Lambda$  is a constant, and  $U(\phi)$  depends on  $\phi$ . Inflation ends due to the presence of a symmetry breaking field  $\chi$ . As long as  $\chi$  is close to 0, the potential can be approximated by Eq. (125) during inflation. The original hybrid model [6] corresponds to  $U(\phi) = m^2\phi^2/2$ , in which case the curvature of the potential is positive ( $V_{,\phi\phi} = m^2 > 0$ ). There is a supersymmetric GUT model with  $U(\phi) = c\Lambda^4 \ln(\phi/\mu)$  [90] (where  $c, \Lambda, \mu$  are positive constants), in which case  $V_{,\phi\phi} = -c\Lambda^4/\phi^2 < 0$ .

We assume that the ratio  $r_U \equiv U(\phi)/\Lambda^4$  is much smaller than 1. For the potential  $V(\phi) = \Lambda^4 + m^2\phi^2/2$ ,  $n_s$  and  $r$  are

$$n_s \simeq 1 + \frac{2m^2 M_{\text{pl}}^2}{\Lambda^4} = 1 + 2\eta_V , \quad r \simeq \frac{8m^4 M_{\text{pl}}^2}{\Lambda^8} \phi^2 \simeq 8(n_s - 1)r_U , \quad (126)$$



in which case  $n_s > 1$ . Under the condition  $r_U < 0.1$ , the tensor-to-scalar ratio is constrained to be  $r < 0.8(n_s - 1)$ . In Fig. 1, the border  $r = 0.8(n_s - 1)$  corresponds to the solid curve in the regime  $n_s > 1$ . Clearly the hybrid model with  $U(\phi) = m^2\phi^2/2 \ll \Lambda^4$  is disfavored from the data.

For the potential  $V(\phi) = \Lambda^4 + c\Lambda^4 \ln(\phi/\mu)$  with  $c \ll 1$ , the number of e-foldings can be estimated as  $N \simeq (\phi^2 - \phi_c^2)/(2M_{\text{pl}}^2 c)$ , where  $\phi_c$  is the field value at the bifurcation point. Using the approximation  $\phi^2 \gg \phi_c^2$ , it follows that

$$n_s \simeq 1 - \frac{2+3c}{2N}, \quad r \simeq \frac{4c}{N} \simeq \frac{8c}{2+3c}(1-n_s), \quad (127)$$

in which case  $n_s < 1$ . For  $0 < c < 0.1$  and  $N = 60$ , the observables (127) are in the ranges  $0.9808 < n_s < 0.9833$  and  $0 < r < 6.67 \times 10^{-3}$ . As we see in Fig. 1, the theoretical curve lies outside the 95 % CL region. Even for  $N = 50$  (which gives smaller values of  $n_s$ ), the model is outside the 95 % CL boundary constrained by the Planck, WP, BAO, and high- $\ell$  data.

#### 4. Very small-field inflation

There are some models in which the variation of the field during inflation is much smaller than  $M_{\text{pl}}$  and hence  $r \ll 0.01$  from Eq. (54). Let us consider the inflaton potential of the form

$$V(\phi) = \Lambda^4[1 - f(\phi)], \quad (128)$$

where  $\Lambda$  is a constant and  $f(\phi)$  is a function of  $\phi$ . The function  $f(\phi) = e^{-\phi/M}$  appears in the context of D-brane inflation [91]. The Kähler-moduli inflation corresponds to the choice  $f(\phi) = c_1\phi^{4/3}e^{-c_2\phi^{4/3}}$  ( $c_1 > 0$ ,  $c_2 > 0$ ) [92]. In both models, the potential  $V(\phi)$  is asymptotically flat in the limit  $\phi \rightarrow \infty$ . There are other potentials of the form  $f(\phi) = (M/\phi)^n$  ( $n > 0$ ) [91, 93] or  $f(\phi) = \lambda_1(\phi - \phi_0) + \lambda_3(\phi - \phi_0)^3/3!$  [94], but these models are generally plagued by the so-called  $\eta$ -problem for the natural parameters constrained by string theory.

Let us consider the case  $f(\phi) = e^{-\phi/M}$ . Then, the number of e-foldings is estimated as  $N \simeq (M/M_{\text{pl}})^2 e^{\phi/M}$ . We also obtain

$$n_s \simeq 1 - \frac{2}{N}, \quad r \simeq \frac{8}{N^2} \left( \frac{M}{M_{\text{pl}}} \right)^2. \quad (129)$$

For  $N = 60$  and  $M < M_{\text{pl}}$ , it follows that  $n_s \simeq 0.967$  and  $r < 2.2 \times 10^{-3}$ . As we see in Fig. 1, this model is inside the 68 % CL boundary constrained by the Planck, WP, BAO, and high- $\ell$  data.

In Kähler-moduli inflation with  $f(\phi) = c_1\phi^{4/3}e^{-c_2\phi^{4/3}}$ , we have that  $0.960 < n_s < 0.967$  and  $r < 10^{-10}$  for  $50 < N < 60$  [92]. This model is well inside the 68 % CL contour.

### B. Non-minimally coupled models

We study the non-minimally coupled models given by the action (58) with  $F(\phi) = 1 - \xi\phi^2/M_{\text{pl}}^2$  and  $\omega = 1$ . Since the same consistency relation as that in standard potential-driven inflation ( $r = -8n_t$ ) holds, the observational constraints in the  $(n_s, r)$  plane are the same as those in Fig. 1. For two potentials  $V(\phi) = m^2\phi^2/2$  and  $V(\phi) = \lambda\phi^4/4$ , we numerically evaluate the observables (63) and (64) for the values of  $x = \phi/M_{\text{pl}}$  corresponding to  $N = 60$ . We focus on the negative non-minimal couplings<sup>1</sup> with which  $r$  gets smaller relative to the case  $\xi = 0$ .

For the potential  $V(\phi) = m^2\phi^2/2$ , the scalar spectral index decreases for larger values of  $|\xi|$  [48, 75, 95]. In Fig. 2, we plot the theoretical values of  $n_s$  and  $r$  as a function of  $\xi$ . From the joint data analysis of Planck+WP+BAO+high- $\ell$ , we obtain the following bounds for  $N = 60$ :

$$-4.2 \times 10^{-3} < \xi < -1.1 \times 10^{-3} \quad (68 \text{ \% CL}), \quad (130)$$

$$-5.1 \times 10^{-3} < \xi \leq 0 \quad (95 \text{ \% CL}). \quad (131)$$

The bound (131) is slightly tighter than  $\xi > -7.0 \times 10^{-3}$  (95 % CL) [48] derived from the WMAP7 data with  $N = 55$ .

---

<sup>1</sup> In our notation the conformal coupling corresponds to  $\xi = 1/6$ .

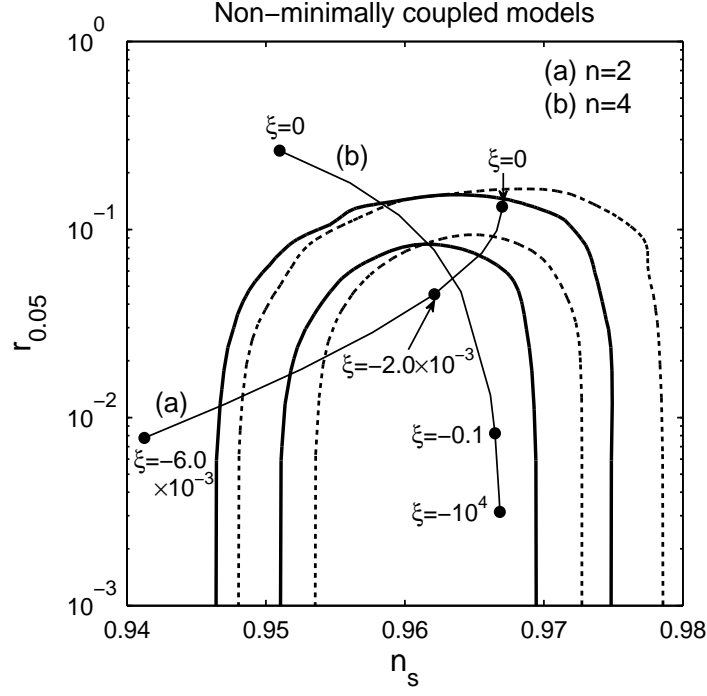


Figure 2: 2-dimensional observational constraints on non-minimally coupled models ( $\xi R\phi^2/2$ ) with  $N = 60$ . The 68 % and 95 % CL observational contours are the same as those given in Fig. 1. The curves (a) and (b) show the theoretical predictions of the potentials  $V(\phi) = m^2\phi^2/2$  and  $V(\phi) = \lambda\phi^4/4$ , respectively, with negative values of  $\xi$ . For larger  $|\xi|$ , the scalar spectral index of the model (a) gets smaller. With the increase of  $|\xi|$ , the model (b) enters the region inside the 68 % CL boundary.

For the potential  $V(\phi) = \lambda\phi^4/4$ , the negative non-minimal couplings lead to the increase of  $n_s$  as well as the decrease of  $r$  [48, 74, 75, 95, 96]. In the limit that  $|\xi| \rightarrow \infty$  with  $N \gg 1$ , the observables (63) and (64) reduce to

$$n_s \simeq 1 - \frac{2}{N}, \quad r \simeq \frac{12}{N^2}. \quad (132)$$

For  $N = 60$ , we have  $n_s = 0.967$  and  $r = 3.33 \times 10^{-3}$ , in which case the model is inside the 68 % CL contour. In this regime, the scalar power spectrum (65) is approximately given by  $\mathcal{P}_{\mathcal{R}} \simeq \lambda N^2 / (72\pi^2 \xi^2)$ . Since the best-fit value of the scalar amplitude at  $k_0 = 0.05 \text{ Mpc}^{-1}$  is  $\mathcal{P}_{\mathcal{R}} = 2.2 \times 10^{-9}$ , it follows that  $\lambda/\xi^2 \simeq 4.3 \times 10^{-10}$ . For the self-coupling  $\lambda = 0.1$ , we have  $\xi \simeq -1.5 \times 10^4$ . In Fig. 2, the theoretical values of  $n_s$  and  $r$  are plotted as a function of  $\xi$ . The bounds on  $\xi$  derived from the joint data analysis of Planck+WP+BAO+high- $\ell$  (for  $N = 60$ ) are

$$\xi < -4.5 \times 10^{-3} \quad (68 \text{ \% CL}), \quad (133)$$

$$\xi < -1.9 \times 10^{-3} \quad (95 \text{ \% CL}), \quad (134)$$

which are slightly tighter than those derived in Refs. [48, 96] with the WMAP7 data. These results are consistent with those of the Planck group [13].

### C. Running kinetic couplings

We proceed to the running kinetic coupling model described by the action (58) with  $F(\phi) = 1$  and  $\omega(\phi) = e^{\mu\phi/M_{\text{Pl}}}$ . For the power-law potential (55), the scalar spectral index and the tensor-to-scalar ratio are given by Eq. (71). For increasing  $\mu$ ,  $n_s$  gets larger, whereas  $r$  decreases. If  $\mu$  is much larger than 1, these observables can be estimated as [48]

$$n_s \simeq 1 - \frac{1}{N}, \quad r \simeq \frac{8n}{N} \frac{1}{\mu x}, \quad (135)$$

where  $N \simeq xe^{\mu x}/(n\mu)$ . In the limit  $\mu \rightarrow \infty$ , the asymptotic values of  $n_s$  and  $r$  are  $n_s \rightarrow 0.983$  and  $r \rightarrow 0$  for  $N = 60$ , respectively. As we see in Fig. 3, the running kinetic coupling model in this limit is outside the 95 % CL contour.

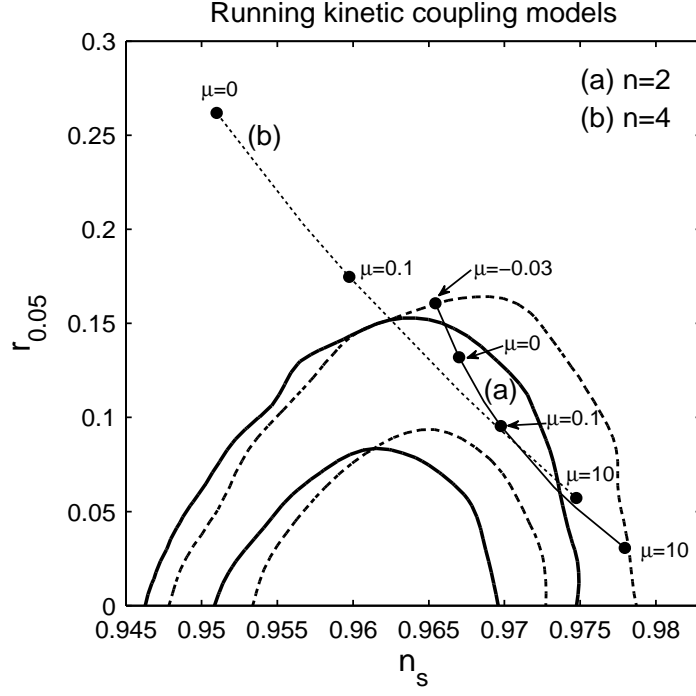


Figure 3: 2-dimensional observational constraints on the running kinetic coupling model ( $\omega(\phi) = e^{\mu\phi/M_{\text{Pl}}}$ ) with  $N = 60$ . The 68 % and 95 % CL observational contours are the same as those given in Fig. 1. The curves (a) and (b) correspond to the cases of the potentials  $V(\phi) = m^2\phi^2/2$  and  $V(\phi) = \lambda\phi^4/4$ , respectively, with  $\mu$  ranging  $-0.03 \leq \mu \leq 10$  ( $n = 2$ ) and  $0 \leq \mu \leq 10$  ( $n = 4$ ). For larger  $\mu$ , the scalar spectral index increases, while the tensor-to-scalar ratio gets smaller.

For the intermediate values of  $\mu$ , however, the models can be within the 95 % CL region even for the potential  $V(\phi) = \lambda\phi^4/4$ . From the joint data analysis of Planck+WP+BAO+high- $\ell$ , we find that  $\mu$  is constrained to be

$$-0.02 < \mu < 0.57 \quad (95\% \text{ CL}) \quad \text{for } n = 2, \quad (136)$$

$$0.18 < \mu < 5.0 \quad (95\% \text{ CL}) \quad \text{for } n = 4. \quad (137)$$

These lower bounds of  $\mu$  are slightly tighter than those derived in Ref. [48] with the WMAP7 data. The WMAP7 data do not put upper bounds of  $\mu$  because even the model with  $n_s = 0.983$  and  $r = 0$  is allowed. With the Planck data, however, the tighter upper limits of  $n_s$  constrain  $\mu$  from above.

#### D. Brans-Dicke theories

We study inflation in Brans-Dicke theories described by the action (73) with the potential (77). In the limit that  $\omega_{\text{BD}} \rightarrow \infty$ , the parameter  $\gamma = 1/\sqrt{3/2 + \omega_{\text{BD}}}$  is close to 0, so that the potential (78) in the Einstein frame is approximated as  $U(\chi) \simeq (3/4)\gamma^2 M^2 \chi^2$ . In this limit,  $n_s$  and  $r$  approach the values (56) of chaotic inflation with  $n = 2$ .

For the theories with  $|\omega_{\text{BD}}| \lesssim \mathcal{O}(1)$ , it follows that  $F_f = 1 + \sqrt{2}\gamma = \mathcal{O}(1)$  and  $N \simeq F/(2\gamma^2)$ . Since  $F \gg 1$  for  $N \gg 1$ , the observables (79) reduce to

$$n_s \simeq 1 - \frac{2}{N}, \quad r \simeq \frac{4(3 + 2\omega_{\text{BD}})}{N^2}. \quad (138)$$

The Starobinsky's model  $f(R) = R + R^2/(6M^2)$  corresponds to  $\omega_{\text{BD}} = 0$ , in which case  $n_s$  and  $r$  are the same as Eq. (132). As we see in Fig. 4, the tensor-to-scalar ratio decreases for smaller  $\omega_{\text{BD}}$  with the asymptotic value  $r \rightarrow 0$  in the limit  $\omega_{\text{BD}} \rightarrow -3/2$ . From the joint data analysis of Planck+WP+BAO+high- $\ell$ , the Brans-Dicke parameter is constrained to be

$$\omega_{\text{BD}} < 11.5 \quad (68\% \text{ CL}). \quad (139)$$

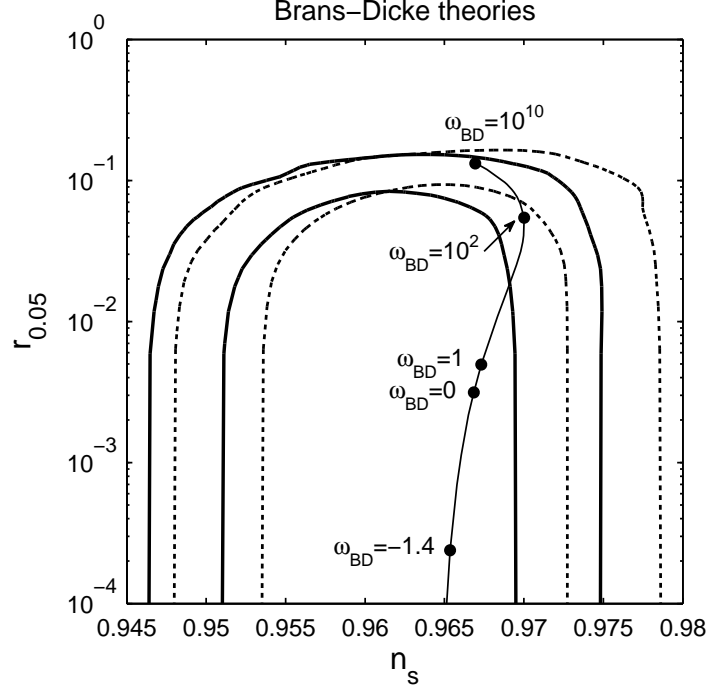


Figure 4: 2-dimensional observational constraints on inflation in Brans-Dicke theories in the presence of the potential (77) with  $N = 60$ . The 68 % and 95 % CL observational contours are the same as those given in Fig. 1. The solid curve shows the theoretical predictions in the regime  $-1.5 < \omega_{\text{BD}} < \infty$ . The Starobinsky's  $f(R)$  model  $f(R) = R + R^2/(6M^2)$  corresponds to the case  $\omega_{\text{BD}} = 0$ .

### E. Potential-driven Galileon inflation

We proceed to the potential-driven Galileon inflation described by the Lagrangian (81). We consider the effects of three covariant Galileon terms  $G_3 = c_3 X/M^3$ ,  $G_4 = -c_4 X^2/M^6$ , and  $G_5 = 3c_5 X^2/M^9$  separately. We study the cases of two power-law potentials  $V(\phi) = \lambda\phi^n/n$  with  $n = 2$  and  $n = 4$  in the regime  $\phi > 0$ . Since  $\dot{\phi} < 0$  during inflation, we can choose the coefficients of the terms  $G_i$  ( $i = 3, 4, 5$ ) to be  $c_3 = -1$ ,  $c_4 = -1$ , and  $c_5 = -1$  without loss of generality (the signs of  $c_i$  are fixed to avoid scalar ghosts). For small  $M$ , there appears a regime in which the Galileon self-interaction dominates over the standard kinetic term during inflation. In the limit that  $M \rightarrow 0$ , the scalar spectral index and the tensor-to-scalar ratio in Eq. (94) reduce to [52, 79]

$$n_s = 1 - \frac{3(n+1)}{(n+3)N+n}, \quad r = \frac{64\sqrt{6}}{9} \frac{n}{(n+3)N+n} \quad (G_3 \text{ dominant}), \quad (140)$$

$$n_s = 1 - \frac{2(5n+4)}{4(n+2)N+3n}, \quad r = \frac{208\sqrt{39}}{27} \frac{n}{4(n+2)N+3n} \quad (G_4 \text{ dominant}), \quad (141)$$

$$n_s = 1 - \frac{7n+5}{(3n+5)N+2n}, \quad r = \frac{256\sqrt{10}}{25} \frac{n}{(3n+5)N+2n} \quad (G_5 \text{ dominant}). \quad (142)$$

We recall that, in this regime, the consistency relations are given by Eqs. (91)-(93) respectively, which are different from  $r = -8n_t$  in standard slow-roll inflation. In Fig. 5, we plot the 68 % and 95 % CL observational contours derived by using the two consistency relations:  $r = -8n_t$  and  $r = -8.709n_t$ . Since they are similar to each other, we can safely use the observational bounds in the  $(n_s, r)$  plane constrained from the standard relation  $r = -8n_t$ .

As we see in Fig. 5,  $n_s$  increases for smaller  $M$ , whereas  $r$  gets smaller. For the potential  $V(\phi) = m^2\phi^2/2$  the theoretical curves lie inside the 95 % CL boundary, but still they are outside the 68 % CL contour. If the Galileon self-interaction dominates over the standard kinetic term even after inflation, there is no oscillatory regime of inflaton during reheating [79]. This is typically accompanied by the appearance of the negative propagation speed squared  $c_s^2$ . This puts lower bounds on  $M$ , e.g.,  $M > 4.2 \times 10^{-4} M_{\text{Pl}}$  for  $G_3 = -X/M^3$ . Even for the values of  $M$  around these lower bounds,  $n_s$  and  $r$  are close to the asymptotic values given in Eqs. (140)-(142).

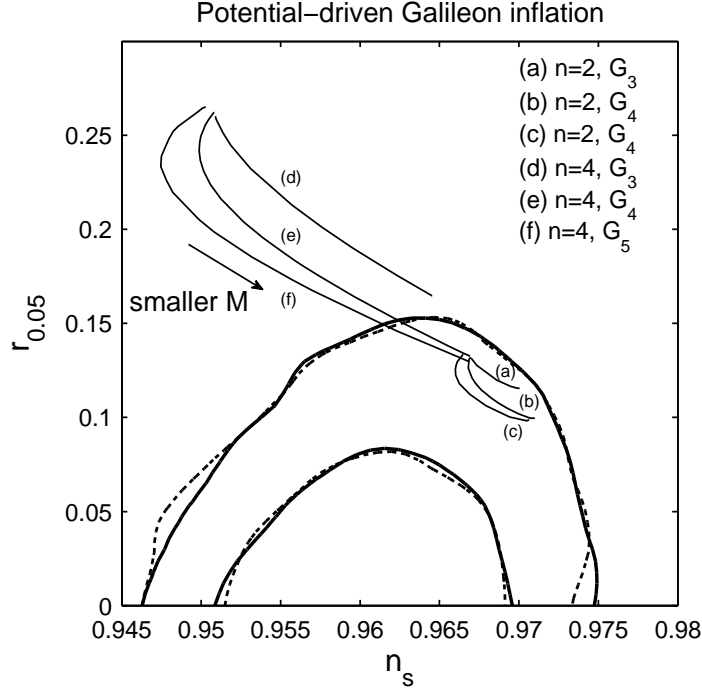


Figure 5: 2-dimensional observational constraints on potential-driven Galileon inflation with  $N = 60$  derived from the joint data analysis of Planck+WP+BAO+high- $\ell$ . The bold solid curves correspond to the 68 % CL (inside) and 95 % CL (outside) contours derived by using the consistency relation  $r = -8n_t$ , whereas the dashed curves show the 68 % and 95 % CL boundaries obtained from the consistency relation  $r = -8.709n_t$ . Each thin solid curve shows the theoretical prediction of the potentials  $V(\phi) = m^2\phi^2/2$  or  $V(\phi) = \lambda\phi^4/4$  in the presence of the terms  $G_3 = -X/M^3$ , or,  $G_4 = X^2/M^6$ , or  $G_5 = -3X^2/M^9$ . For smaller  $M$ , the tensor-to-scalar ratio decreases.

For the potential  $V(\phi) = \lambda\phi^4/4$  with the term  $G_3 = -X/M^3$ , the asymptotic values in Eq. (140) are  $n_s = 0.965$  and  $r = 0.164$  for  $N = 60$ . Because of the large tensor-to-scalar ratio, this model is outside the 95 % CL contour for arbitrary values of  $M$ . In the presence of the terms  $G_4 = X^2/M^6$  or  $G_5 = -3X^2/M^9$ , there are some values of  $M$  with which the potential  $V(\phi) = \lambda\phi^4/4$  enters the 95 % CL region. From the joint analysis of Planck+WP+BAO+high- $\ell$ , we obtain the following bounds

$$M < 7.2 \times 10^{-4} M_{\text{pl}} \quad (95 \text{ \% CL}) \quad (G_4 \text{ dominant}), \quad (143)$$

$$M < 6.6 \times 10^{-4} M_{\text{pl}} \quad (95 \text{ \% CL}) \quad (G_5 \text{ dominant}), \quad (144)$$

which are tighter than those derived with the WMAP7 data:  $M < 1.1 \times 10^{-3} M_{\text{pl}}$  ( $G_4$  dominant) and  $M < 8.6 \times 10^{-4} M_{\text{pl}}$  ( $G_5$  dominant) [79]. In order to avoid the negative values of  $c_s^2$ , we require that  $M > 2.3 \times 10^{-4} M_{\text{pl}}$  ( $G_4$  dominant) and  $M > 2.9 \times 10^{-4} M_{\text{pl}}$  ( $G_5$  dominant) [79]. Hence there are still allowed parameter spaces compatible with the bounds (143) and (144).

### F. Field-derivative couplings to the Einstein tensor

The model with the field derivative couplings to the Einstein tensor is given by the action (99). In this case, the consistency relation (101) is the same as that in standard slow-roll inflation. In the following, we focus on the two potentials  $V(\phi) = \lambda\phi^n/n$  with  $n = 2$  and  $n = 4$ . In the limit that  $M \rightarrow 0$  (i.e.,  $\alpha = \lambda M_{\text{pl}}^{n-2}/M^2 \rightarrow \infty$ ), the observables in Eq. (102) reduce to [80]

$$n_s = 1 - \frac{4(n+1)}{2(n+2)N+n}, \quad r = \frac{16n}{2(n+2)N+n}. \quad (145)$$

When  $N = 60$ , we have  $n_s = 0.975$ ,  $r = 0.066$  for  $n = 2$  and  $n_s = 0.972$ ,  $r = 0.088$  for  $n = 4$ .

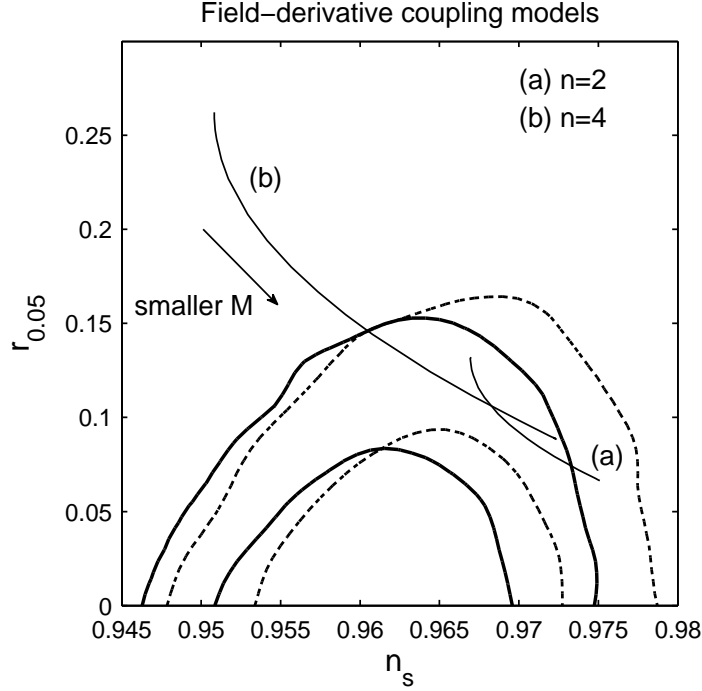


Figure 6: 2-dimensional observational constraints on field-derivative coupling models with  $N = 60$ . The 68 % and 95 % CL observational contours are the same as those given in Fig. 1. The thin-solid curves correspond to the theoretical predictions of the potentials  $V(\phi) = m^2\phi^2/2$  and  $V(\phi) = \lambda\phi^4/4$ , respectively, in the presence of the term  $G^{\mu\nu}\partial_\mu\phi\partial_\nu\phi/(2M^2)$ . The tensor-to-scalar ratio gets smaller for decreasing  $M$ .

In Fig. 6, we plot the theoretical values of  $n_s$  and  $r$  as a function of  $M$  for  $n = 2$  and  $n = 4$ . Even in the presence of the field-derivative couplings, both potentials are outside the 68 % CL region. For the potential  $V(\phi) = m^2\phi^2/2$ , the model with the asymptotic values (145) lies outside the 95 % CL region constrained by the Planck, WP, BAO, and high- $\ell$  data. This puts an upper bound on the parameter  $\alpha$ , as  $\alpha < 0.3$  (95 % CL). On the other hand, from the joint analysis of Planck+WP+BAO, the theoretical curve is still inside the 95 % CL contour.

For the potential  $V(\phi) = \lambda\phi^4/4$ , the model with the asymptotic values (145) is marginally inside the 95 % CL boundary constrained from the Planck, WP, BAO, and high- $\ell$  data. This potential is within the 95 % CL region for

$$\alpha = \lambda M_{\text{pl}}^2/M^2 > 9.0 \times 10^{-5}. \quad (146)$$

This bound is tighter than  $\alpha > 3.0 \times 10^{-5}$  derived by using the WMAP7 data [80].

## G. k-inflation

### 1. Dilatonic ghost condensate

The dilatonic ghost condensate model is given by the Lagrangian (111). Using the formulas of  $n_s$ ,  $n_t$ , and  $r$  given in Eq. (112), we carry out the likelihood analysis by varying  $c_s$  in the range  $0 \leq c_s \leq 1$  together with other cosmological parameters. In Fig. 7, we plot the 1-dimensional marginalized probability distributions of  $c_s$  derived from the joint data analyses of Planck+WP+BAO+high- $\ell$  (solid curve) and Planck+WP+BAO (dotted curve). The Planck+WP+BAO+high- $\ell$  data give the following constraints

$$0.038 < c_s < 0.043 \quad (68 \text{ \% CL}), \quad (147)$$

$$0.034 < c_s < 0.046 \quad (95 \text{ \% CL}). \quad (148)$$

We also obtain similar bounds from the joint analysis of Planck+WP+BAO. Since the Harrison-Zeldovich spectrum ( $n_s = 1$ ,  $r = 0$ ) is disfavored from the data, the model with  $c_s = 0$  is outside the 95 % CL boundary.

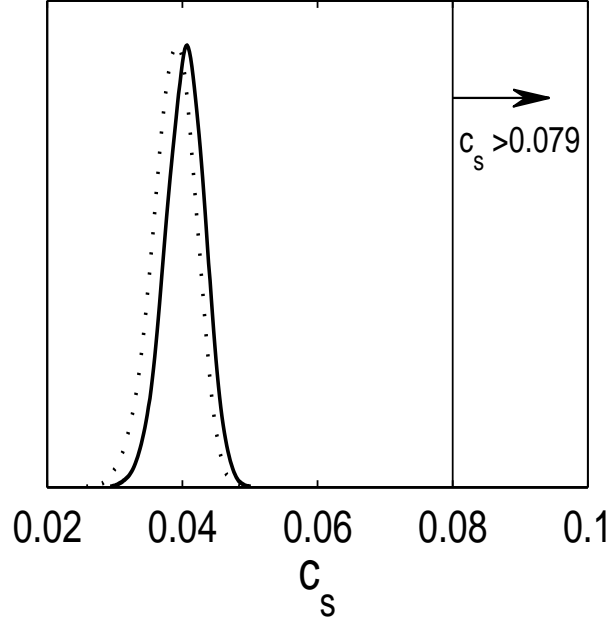


Figure 7: 1-dimensional marginalized probability distribution (solid curve) of the scalar propagation speed  $c_s$  constrained by the Planck, WP, BAO, and high- $\ell$  data in the dilatonic ghost condensate model. The dotted curve shows the probability distribution of  $c_s$  derived from the Planck, WP, and BAO data. The analysis of the non-Gaussianity puts the further bound  $c_s > 0.079$ , by which the model is excluded at more than 95 % CL.

For  $c_s \ll 1$ , the non-linear estimator at the equilateral triangle given in Eq. (112) satisfies  $|f_{\text{NL}}^{\text{eq}}| \gg 1$ . Hence there should be a lower bound of  $c_s$ . In order to compare the model prediction with the observations of non-Gaussianities, we need to employ the leading-order bispectrum given by Eq. (42). For the dilatonic ghost condensate model the bispectrum reads

$$\mathcal{A}_{\mathcal{R}}^{\text{lead}} = -\frac{13}{288} \left( \frac{1}{c_s^2} - 1 \right) [2 + 3\beta + c_s^2(3\beta - 2)] S_7^{\text{equil}} + \frac{1}{96} \left( \frac{1}{c_s^2} - 1 \right) (1 + c_s^2)(13\beta - 14) S_7^{\text{ortho}}. \quad (149)$$

In the limit  $c_s^2 \ll 1$ , it follows that  $\mathcal{A}_{\mathcal{R}} \simeq (-0.252/c_s^2) S_7^{\text{equil}} + 0.016 S_7^{\text{ortho}}$  and hence the equilateral shape dominates over the orthogonal one. The Planck team used the equilateral template introduced in Ref. [97] for the above model (equivalent to “power-law k-inflation” of Ref. [24]) and derived the following bound

$$c_s > 0.079 \quad (95 \text{ \% CL}). \quad (150)$$

This is not compatible with the constraint (148), so the dilatonic ghost condensate model is severely disfavored. The same conclusion was reached in Ref. [24], but we derived more precise bounds (147)-(148) by performing the joint data analysis of Planck+WP+BAO+high- $\ell$ .

## 2. DBI model

The DBI model with power-law inflation is given by the Lagrangian (113) with the functions (114). Using the formulas (116), we vary two parameters  $c_s$  and  $n_s$  in the ranges  $0 < c_s \leq 1$  and  $0.90 \leq n_s \leq 1$ . When  $c_s = 0$ , we have  $\tilde{Y} = 1/2$  and  $\epsilon = 3/2$  from Eq. (115), in which case inflation is not realized. Even for  $c_s \ll 1$ , as long as  $c_s$  is not exactly 0, it is possible to find the large parameter  $c_M$  satisfying the condition  $c_M c_s \gg 1$ . Then,  $|n_s - 1|$  can be much smaller than 1 to match with the observational data.

In Fig. 8, we plot the 68% and 95% CL observational contours derived from the joint data analysis of Planck+WP+BAO+high- $\ell$  and Planck+WP+BAO. From the Planck+WP+BAO+high- $\ell$  data, the scalar propagation speed is constrained to be

$$0 < c_s < 0.17 \quad (68 \text{ \% CL}), \quad (151)$$

$$0 < c_s < 0.43 \quad (95 \text{ \% CL}). \quad (152)$$



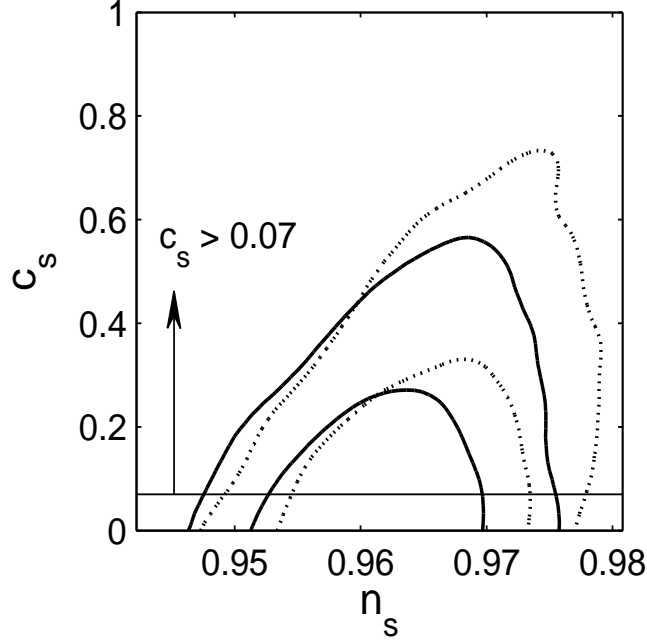


Figure 8: 2-dimensional observational constraints in the  $(n_s, c_s)$  plane in the DBI model with power-law inflation. The bold solid curves show the 68 % CL (inside) and 95 % CL (outside) boundaries derived by the joint data analysis of Planck+WP+BAO+high- $\ell$ , whereas the dotted curves are the 68 % and 95 % contours constrained by Planck+WP+BAO. We also show the bound  $c_s > 0.07$  coming from the non-Gaussianity.

The upper bounds of  $c_s$  come from the fact, for  $c_s^2$  close to 1, the spectrum approaches the Harrison-Zeldovich one. If we do not include the high- $\ell$  data, the upper limits of  $c_s$  are slightly weaker. When  $c_s \ll 1$ , the observationally allowed values of  $n_s$  are similar to those shown in Fig. 1 for  $r \ll 1$ . In the regime  $0 < c_s \ll 1$ , the scalar spectral index can be compatible with the data due to the presence of the exponential potential satisfying  $c_M c_s \gg 1$ .

In the DBI model, the non-linear estimator at the equilateral triangle is given by  $f_{\text{NL}}^{\text{eq}} = -(35/108)(1/c_s^2 - 1)$  and hence  $|f_{\text{NL}}^{\text{eq}}| \gg 1$  for  $c_s \ll 1$ . The leading-order bispectrum (42) reads

$$\mathcal{A}_{\mathcal{R}}^{\text{lead}} = -\frac{13\beta}{48} \left( \frac{1}{c_s^2} - 1 \right) S_7^{\text{equil}} + \frac{13\beta - 14}{48} \left( \frac{1}{c_s^2} - 1 \right) S_7^{\text{ortho}}. \quad (153)$$

In the limit  $c_s^2 \ll 1$ , we have  $\mathcal{A}_{\mathcal{R}} \simeq (-0.324/c_s^2) S_7^{\text{equil}} + 0.0325 S_7^{\text{ortho}}$ , in which case the orthogonal shape provides some contribution to the total bispectrum. The Planck team used the shape function of the DBI model introduced in Ref. [64] and obtained the following bound [24]

$$c_s > 0.07 \quad (95\% \text{ CL}). \quad (154)$$

Since the bispectrum (153) is valid for any function of  $f(\phi)$  and  $V(\phi)$  in Eq. (113), we can use the constraint (154) for our power-law DBI model as well. Combining (154) with the bound (152), the scalar propagation speed is constrained to be  $0.07 < c_s < 0.43$  (95 % CL).

## V. CONCLUSIONS

We have studied observational constraints on single-field inflation in the framework of the Horndeski's most general scalar-tensor theories. This covers a wide class of gravitational theories such as (i) a canonical field with a potential, (ii) a non-minimally coupled scalar field with the Ricci scalar  $R$ , (iii) running kinetic couplings  $\omega(\phi)X$ , (iv) Brans-Dicke theories (including  $f(R)$  gravity), (v) potential-driven Galileon inflation, (vi) field-derivative couplings  $G^{\mu\nu} \partial_\mu \phi \partial_\nu \phi$  to the Einstein tensor, and (vii) k-inflation. Under the slow-variation approximation the inflationary observables like  $n_s$ ,  $r$ ,  $n_t$ , and  $f_{\text{NL}}$  can be evaluated in a unified way for the general action (1).

With the recent Planck data, we run the CosmoMC code by assuming the flat  $\Lambda$ CDM Universe. Since the scalar and tensor runnings are of the order of  $\epsilon^2$  under the slow-variation approximation, we set these parameters to be 0

in the likelihood analysis. The consistency relation between  $r(k_0)$  and  $n_t(k_0)$  is different depending on the models, so we vary the inflationary observables  $\mathcal{P}_{\mathcal{R}}(k_0)$ ,  $n_s(k_0)$ , and  $r(k_0)$  after deriving the consistency relation in each model.

The difference from the data analysis of the Planck team [13] is that we carried out the joint observational constraints with the Planck, WP, BAO, and high- $\ell$  data by taking the pivot wave number  $k_0 = 0.05 \text{ Mpc}^{-1}$  (unlike  $k_0 = 0.002 \text{ Mpc}^{-1}$  used by the Planck team). We confirmed that the joint analysis of Planck, WP, and BAO with the consistency relation  $r(k_0) = -8n_t(k_0)$  reproduces the results presented in Ref. [13] very well. By adding the high- $\ell$  data, we find that the upper bound of  $n_s$  becomes tighter than that derived in Fig. 1 of Ref. [13] (which is based on either “Planck+WP+BAO” or “Planck+WP+high- $\ell$ ”).

For each inflationary scenario studied in this paper, we summarize the main results as follows.

- (i) A canonical field with a potential  $V(\phi)$

Chaotic inflation with the quadratic potential  $V(\phi) = m^2\phi^2/2$  is marginally inside the 95 % CL region. From the joint data analysis of Planck+WP+BAO+high- $\ell$ , the potentials  $V(\phi) = \lambda\phi^n/n$  with  $n = 1$  and  $n = 2/3$  are outside the 95 % CL boundary for  $N = 60$ . The constraints on the models  $n = 1$  and  $n = 2/3$  are tighter than those derived by the Planck team [13].

In Natural inflation, the symmetry breaking scale  $f$  is constrained to be  $5.1M_{\text{pl}} < f < 7.9M_{\text{pl}}$  (68 % CL) and  $f > 4.6M_{\text{pl}}$  (95 % CL). The upper bound of  $f$  was newly derived.

Hybrid inflation with the potential  $V(\phi) = \Lambda^4 + m^2\phi^2/2$  is disfavored from the data in the regime  $\Lambda^4 \gg m^2\phi^2/2$ . In another Hybrid inflation model with the potential  $V(\phi) = \Lambda^4[1 + c\ln(\phi/\mu)]$ , the scalar spectral index can be as small as  $n_s = 0.98$  with a suppressed tensor-to-scalar ratio, but such a model is outside the 95 % CL contour. These confirm the results of Ref. [13].

We also studied the potentials of the form  $V(\phi) = \Lambda^4[1 - f(\phi)]$ , where  $f(\phi)$  is a function that asymptotically approaches 0 in the limit  $\phi \rightarrow \infty$ . For the functions  $f(\phi) = e^{-\phi/M}$  and  $f(\phi) = c_1\phi^{4/3}e^{-c_2\phi^{4/3}}$  appearing in D-brane inflation and Kähler-moduli inflation respectively, we have  $n_s \simeq 1 - 2/N$  with a very small tensor-to-scalar ratio. Such models are most favored observationally.

- (ii) Non-minimally coupled models with  $\xi\phi^2R/2$

For the quadratic potential  $V(\phi) = m^2\phi^2/2$ , we derived the new bound  $-4.2 \times 10^{-3} < \xi < -1.1 \times 10^{-3}$  (68 % CL). The quartic potential  $V(\phi) = \lambda\phi^4/4$  enters the 68 % CL region for  $\xi < -4.5 \times 10^{-3}$  (which is consistent with the result of Ref. [13]). In Higgs inflation, we have  $n_s \simeq 1 - 2/N$  and  $r \simeq 12/N^2$  in the limit  $|\xi| \rightarrow \infty$ , in which case the model is well inside the 68 % CL region.

- (iii) Running kinetic couplings  $\omega(\phi)X$

The coupling  $\omega(\phi) = e^{\mu\phi/M_{\text{pl}}}$  ( $\mu > 0$ ) can reduce the tensor-to-scalar ratio for the potential  $V(\phi) = \lambda\phi^n/n$  ( $n > 0$ ). In the limit  $\mu \gg 1$ , however,  $n_s \simeq 1 - 1/N = 0.983$  for  $N = 60$ , in which case the model is outside the 95 % CL region. We derived the new bounds  $-0.02 < \mu < 0.57$  (95 % CL) for  $n = 2$  and  $0.18 < \mu < 5.0$  (95 % CL) for  $n = 4$ .

- (iv) Brans-Dicke theories

In Brans-Dicke theories, the potential  $V(\phi) = (3M^2/4)(\phi - M_{\text{pl}})^2$  reproduces the Starobinsky’s model  $f(R) = R + R^2/(6M^2)$  for  $\omega_{\text{BD}} = 0$ . We test inflation in BD theories for the same potential with arbitrary BD parameters  $\omega_{\text{BD}}$ . For  $|\omega_{\text{BD}}| \lesssim 1$ , we have  $n_s \simeq 1 - 2/N$  and  $r \simeq 4(3 + 2\omega_{\text{BD}})/N^2$ . The BD parameter is constrained to be  $\omega_{\text{BD}} < 11.5$  (68 % CL).

- (v) Potential-driven Galileon inflation

With the Galileon self-interactions  $G_3 = -X/M^3$ ,  $G_4 = X^2/M^6$ ,  $G_5 = -3X^2/M^9$ , the tensor-to-scalar ratio can get smaller relative to the case of standard potential-driven inflation. For the quadratic potential  $V(\phi) = m^2\phi^2/2$ , the model is inside the 95 % CL contour, but outside the 68 % CL region for  $N = 60$ . The quartic potential  $V(\phi) = \lambda\phi^4/4$  with  $G_3 = -X/M^3$  is outside the 95 % CL region for  $N = 60$ . In the presence of the terms  $G_4 = X^2/M^6$  or  $G_5 = -3X^2/M^9$ , however, there are some parameter spaces in which the quartic potential is inside the 95 % CL boundary.

- (vi) Field-derivative couplings  $G^{\mu\nu}\partial_\mu\phi\partial_\nu\phi/(2M^2)$

In the presence of the field-derivative couplings to the Einstein tensor, the tensor-to-scalar ratio reduces as in the case of potential-driven Galileon inflation. However, the potentials  $V(\phi) = \lambda\phi^n/n$  with  $n = 2$  and  $n = 4$  are outside the 68 % CL region. We find that the parameter  $\alpha = \lambda M_{\text{pl}}^{n-2}/M^2$  is constrained to be  $\alpha < 0.3$  for  $n = 2$  and  $\alpha > 9.0 \times 10^{-5}$  for  $n = 4$  at 95 % CL.

- (vii) K-inflation

We studied the power-law k-inflation scenario described by the Lagrangian (105), in which case  $c_s$  is constant. In the dilatonic ghost condensate model, the observables  $n_s$ ,  $n_t$ , and  $r$  are expressed in terms of  $c_s$  alone. From the joint data analysis of Planck+WP+BAO+high- $\ell$ , we derived the bound  $0.034 < c_s < 0.046$  (95 % CL). This is not compatible with the bound  $c_s > 0.079$  (95 % CL) coming from the non-Gaussianity with an equilateral template. In the DBI model with power-law inflation, there are two model parameters  $c_s$  and  $c_M$  in the expressions of  $n_s$ ,  $n_t$ , and  $r$ . In this case, the scalar propagation speed is constrained to be  $0 < c_s < 0.43$  (95 % CL). Since the bound of  $c_s$  coming from the non-Gaussianity is  $c_s > 0.07$  (95 % CL), there are some allowed parameter spaces compatible with both constraints.

The above results show that the models with  $n_s \simeq 1 - 2/N$  and the suppressed tensor-to-scalar ratio are most favored observationally. These include D-brane/Kähler-moduli inflation, non-minimally coupled Higgs inflation, and Brans-Dicke theory in the presence of the potential  $V(\phi) = (3M^2/4)(\phi - M_{\text{pl}})^2$  with the BD parameter  $\omega_{\text{BD}} < \mathcal{O}(1)$ . In natural inflation and non-minimally coupled models with the potential  $V(\phi) = m^2\phi^2/2$ , there are also some allowed parameter spaces inside the 68 % CL region. Most of other models studied in this paper are outside the 68 % CL boundary.

Although we have focused on the single-field models in the framework of Horndeski's theories, there are other single-field inflationary scenarios based on braneworld [98], non-commutative space-time [99], and loop quantum gravity [100]. We leave observational constraints on those models for future work.

### ACKNOWLEDGEMENTS

We thank Nicola Bartolo for useful correspondence. J. O. and S. T. are supported by the Scientific Research Fund of the JSPS (Nos. 23·6781 and 24540286). S. T. also thanks financial support from Scientific Research on Innovative Areas (No. 21111006). S. K. is supported by the Grant-in-Aid for Scientific research No. 24740149.

- 
- [1] A. A. Starobinsky, Phys. Lett. B **91**, 99 (1980).
  - [2] K. Sato, Mon. Not. R. Astron. Soc. **195**, 467 (1981);  
K. Sato, Phys. Lett. **99B**, 66 (1981);  
D. Kazanas, Astrophys. J. **241** L59 (1980);  
A. H. Guth, Phys. Rev. D **23**, 347 (1981).
  - [3] A. D. Linde, Phys. Lett. B **108**, 389 (1982);  
A. Albrecht and P. J. Steinhardt, Phys. Rev. Lett. **48**, 1220 (1982).
  - [4] A. D. Linde, Phys. Lett. B **129**, 177 (1983).
  - [5] K. Freese, J. A. Frieman and A. V. Olinto, Phys. Rev. Lett. **65**, 3233 (1990);  
F. C. Adams, J. R. Bond, K. Freese, J. A. Frieman and A. V. Olinto, Phys. Rev. D **47**, 426 (1993) [hep-ph/9207245].
  - [6] A. D. Linde, Phys. Rev. D **49**, 748 (1994) [astro-ph/9307002].
  - [7] J. E. Lidsey *et al.*, Rev. Mod. Phys. **69** (1997) 373 [astro-ph/9508078];  
D. H. Lyth and A. Riotto, Phys. Rept. **314**, 1 (1999) [hep-ph/9807278];  
B. A. Bassett, S. Tsujikawa and D. Wands, Rev. Mod. Phys. **78**, 537 (2006) [astro-ph/0507632];  
D. Baumann, arXiv:0907.5424 [hep-th].
  - [8] V. F. Mukhanov and G. V. Chibisov, JETP Lett. **33**, 532 (1981);  
A. H. Guth and S. Y. Pi, Phys. Rev. Lett. **49** (1982) 1110;  
S. W. Hawking, Phys. Lett. B **115**, 295 (1982);  
A. A. Starobinsky, Phys. Lett. B **117** (1982) 175;  
J. M. Bardeen, P. J. Steinhardt and M. S. Turner, Phys. Rev. D **28**, 679 (1983).
  - [9] G. F. Smoot *et al.*, Astrophys. J. **396**, L1 (1992).
  - [10] D. N. Spergel *et al.* [WMAP Collaboration], Astrophys. J. Suppl. **148**, 175 (2003) [astro-ph/0302209].
  - [11] P. A. R. Ade *et al.* [Planck Collaboration], arXiv:1303.5076 [astro-ph.CO].
  - [12] G. Hinshaw *et al.* [WMAP Collaboration], arXiv:1212.5226 [astro-ph.CO].
  - [13] P. A. R. Ade *et al.* [Planck Collaboration], arXiv:1303.5082 [astro-ph.CO].
  - [14] T. Suyama, T. Takahashi, M. Yamaguchi and S. Yokoyama, arXiv:1303.5374 [astro-ph.CO];  
Y. -Z. Ma, Q. -G. Huang and X. Zhang, arXiv:1303.6244 [astro-ph.CO];  
T. Kobayashi, F. Takahashi, T. Takahashi and M. Yamaguchi, arXiv:1303.6255 [astro-ph.CO];  
K. Nakayama, F. Takahashi and T. T. Yanagida, arXiv:1303.7315 [hep-ph];  
J. Ohashi, J. Soda and S. Tsujikawa, Phys. Rev. D **87**, 083520 (2013) [arXiv:1303.7340 [astro-ph.CO]];  
D. I. Kaiser and E. I. Sfakianakis, arXiv:1304.0363 [astro-ph.CO];

- A. Ijjas, P. J. Steinhardt and A. Loeb, arXiv:1304.2785 [astro-ph.CO];  
 S. Avila, J. Martin and D. Steer, arXiv:1304.3262 [hep-th];  
 N. Li and X. Zhang, arXiv:1304.4358 [astro-ph.CO];  
 C. Pallis and Q. Shafi, arXiv:1304.5202 [hep-ph].
- [15] D. S. Salopek and J. R. Bond, Phys. Rev. D **42**, 3936 (1990);  
 A. Gangui, F. Lucchin, S. Matarrese and S. Mollerach, Astrophys. J. **430**, 447 (1994);  
 L. Verde, L. M. Wang, A. Heavens and M. Kamionkowski, Mon. Not. Roy. Astron. Soc. **313**, L141 (2000) [astro-ph/9906301].
- [16] E. Komatsu and D. N. Spergel, Phys. Rev. **D63**, 063002 (2001).
- [17] N. Bartolo, S. Matarrese, A. Riotto, Phys. Rev. **D65**, 103505 (2002) [hep-ph/0112261];  
 N. Bartolo, E. Komatsu, S. Matarrese and A. Riotto, Phys. Rept. **402**, 103 (2004) [astro-ph/0406398].
- [18] J. M. Maldacena, JHEP **0305**, 013 (2003) [astro-ph/0210603].
- [19] P. Creminelli and M. Zaldarriaga, JCAP **0410**, 006 (2004) [astro-ph/0407059].
- [20] X. Chen, M. -x. Huang, S. Kachru and G. Shiu, JCAP **0701**, 002 (2007) [hep-th/0605045].
- [21] C. Cheung, A. L. Fitzpatrick, J. Kaplan and L. Senatore, JCAP **0802**, 021 (2008) [arXiv:0709.0295 [hep-th]].
- [22] A. De Felice and S. Tsujikawa, JCAP **1303**, 030 (2013) [arXiv:1301.5721 [hep-th]].
- [23] C. L. Bennett *et al.*, arXiv:1212.5225 [astro-ph.CO].
- [24] P. A. R. Ade *et al.* [Planck Collaboration], arXiv:1303.5084 [astro-ph.CO].
- [25] C. Armendariz-Picon, T. Damour and V. F. Mukhanov, Phys. Lett. B **458**, 209 (1999) [hep-th/9904075].
- [26] J. Garriga and V. F. Mukhanov, Phys. Lett. B **458**, 219 (1999) [hep-th/9904176].
- [27] A. Nicolis, R. Rattazzi and E. Trincherini, Phys. Rev. D **79**, 064036 (2009) [arXiv:0811.2197 [hep-th]].
- [28] C. Deffayet, G. Esposito-Farese and A. Vikman, Phys. Rev. D **79**, 084003 (2009) [arXiv:0901.1314 [hep-th]];  
 C. Deffayet, S. Deser and G. Esposito-Farese, Phys. Rev. D **80**, 064015 (2009) [arXiv:0906.1967 [gr-qc]].
- [29] S. Weinberg, Phys. Rev. D **77**, 123541 (2008) [arXiv:0804.4291 [hep-th]].
- [30] C. Cheung, P. Creminelli, A. L. Fitzpatrick, J. Kaplan and L. Senatore, JHEP **0803**, 014 (2008) [arXiv:0709.0293 [hep-th]].
- [31] D. Seery and J. E. Lidsey, JCAP **0506**, 003 (2005) [astro-ph/0503692].
- [32] X. Chen, B. Hu, M. -x. Huang, G. Shiu and Y. Wang, JCAP **0908**, 008 (2009) [arXiv:0905.3494 [astro-ph.CO]].
- [33] L. Senatore, K. M. Smith and M. Zaldarriaga, JCAP **1001**, 028 (2010) [arXiv:0905.3746 [astro-ph.CO]].
- [34] S. Mizuno and K. Koyama, Phys. Rev. D **82**, 103518 (2010) [arXiv:1009.0677 [hep-th]].
- [35] A. De Felice and S. Tsujikawa, JCAP **1104**, 029 (2011) [arXiv:1103.1172 [astro-ph.CO]].
- [36] T. Kobayashi, M. Yamaguchi and J. 'i. Yokoyama, Phys. Rev. D **83**, 103524 (2011) [arXiv:1103.1740 [hep-th]].
- [37] X. Gao and D. A. Steer, JCAP **1112**, 019 (2011) [arXiv:1107.2642 [astro-ph.CO]].
- [38] A. De Felice and S. Tsujikawa, Phys. Rev. D **84**, 083504 (2011) [arXiv:1107.3917 [gr-qc]].
- [39] G. W. Horndeski, Int. J. Theor. Phys. **10**, 363-384 (1974).
- [40] C. Deffayet, X. Gao, D. A. Steer and G. Zahariade, Phys. Rev. D **84**, 064039 (2011) [arXiv:1103.3260 [hep-th]].
- [41] C. Charmousis, E. J. Copeland, A. Padilla and P. M. Saffin, Phys. Rev. Lett. **108**, 051101 (2012) [arXiv:1106.2000 [hep-th]].
- [42] <http://cosmologist.info/cosmomc/>
- [43] M. Ostrogradski, Mem. Ac. St. Petersburg VI 4, 385 (1850).
- [44] T. Futamase and K. -i. Maeda, Phys. Rev. D **39**, 399 (1989).
- [45] R. Fakir and W. G. Unruh, Phys. Rev. D **41**, 1783 (1990).
- [46] F. L. Bezrukov and M. Shaposhnikov, Phys. Lett. B **659**, 703 (2008) [arXiv:0710.3755 [hep-th]].
- [47] K. Nakayama and F. Takahashi, JCAP **1011**, 009 (2010) [arXiv:1008.2956 [hep-ph]].
- [48] A. De Felice, S. Tsujikawa, J. Elliston and R. Tavakol, JCAP **1108**, 021 (2011) [arXiv:1105.4685 [astro-ph.CO]].
- [49] C. Brans and R. H. Dicke, Phys. Rev. **124**, 925 (1961).
- [50] T. Kobayashi, M. Yamaguchi and J. 'i. Yokoyama, Phys. Rev. Lett. **105**, 231302 (2010) [arXiv:1008.0603 [hep-th]].
- [51] C. Burrage, C. de Rham, D. Seery and A. J. Tolley, JCAP **1101**, 014 (2011) [arXiv:1009.2497 [hep-th]].
- [52] K. Kamada, T. Kobayashi, M. Yamaguchi and J. 'i. Yokoyama, Phys. Rev. D **83**, 083515 (2011) [arXiv:1012.4238 [astro-ph.CO]];  
 K. Kamada, T. Kobayashi, T. Takahashi, M. Yamaguchi and J. 'i. Yokoyama, Phys. Rev. D **86**, 023504 (2012) [arXiv:1203.4059 [hep-ph]].
- [53] L. Amendola, Phys. Lett. B **301**, 175 (1993) [gr-qc/9302010].
- [54] C. Germani and A. Kehagias, Phys. Rev. Lett. **105**, 011302 (2010) [arXiv:1003.2635 [hep-ph]];  
 C. Germani and A. Kehagias, Phys. Rev. Lett. **106**, 161302 (2011) [arXiv:1012.0853 [hep-ph]].
- [55] T. Kobayashi, M. Yamaguchi and J. 'i. Yokoyama, Prog. Theor. Phys. **126**, 511 (2011) [arXiv:1105.5723 [hep-th]].
- [56] X. Gao, T. Kobayashi, M. Yamaguchi and J. 'i. Yokoyama, Phys. Rev. Lett. **107**, 211301 (2011) [arXiv:1108.3513 [astro-ph.CO]].
- [57] F. Beutler *et al.*, Mon. Not. Roy. Astron. Soc. **416**, 3017 (2011) [arXiv:1106.3366 [astro-ph.CO]].
- [58] N. Padmanabhan *et al.*, arXiv:1202.0090 [astro-ph.CO].
- [59] L. Anderson *et al.*, Mon. Not. Roy. Astron. Soc. **427**, no. 4, 3435 (2013) [arXiv:1203.6594 [astro-ph.CO]].
- [60] S. Das *et al.*, arXiv:1301.1037 [astro-ph.CO].
- [61] C. L. Reichardt *et al.*, Astrophys. J. **755**, 70 (2012) [arXiv:1111.0932 [astro-ph.CO]].
- [62] F. Piazza and S. Tsujikawa, JCAP **0407**, 004 (2004) [hep-th/0405054].
- [63] E. Silverstein and D. Tong, Phys. Rev. D **70**, 103505 (2004) [hep-th/0310221].



- [64] M. Alishahiha, E. Silverstein and D. Tong, Phys. Rev. D **70**, 123505 (2004) [hep-th/0404084].
- [65] J. Ohashi and S. Tsujikawa, Phys. Rev. D **83**, 103522 (2011) [arXiv:1104.1565 [astro-ph.CO]].
- [66] A. R. Liddle and S. M. Leach, Phys. Rev. D **68**, 103503 (2003) [astro-ph/0305263].
- [67] R. L. Arnowitt, S. Deser and C. W. Misner, Phys. Rev. **117**, 1595 (1960).
- [68] F. Arroja, A. E. Romano and M. Sasaki, Phys. Rev. D **84**, 123503 (2011) [arXiv:1106.5384 [astro-ph.CO]];  
P. Adshead, C. Dvorkin, W. Hu and E. A. Lim, Phys. Rev. D **85**, 023531 (2012) [arXiv:1110.3050 [astro-ph.CO]];  
M. H. Namjoo, H. Firouzjahi and M. Sasaki, Europhys. Lett. **101**, 39001 (2013) [arXiv:1210.3692 [astro-ph.CO]];  
X. Chen, H. Firouzjahi, M. H. Namjoo and M. Sasaki, arXiv:1301.5699 [hep-th].
- [69] D. H. Lyth, Phys. Rev. Lett. **78**, 1861 (1997) [hep-ph/9606387].
- [70] F. Lucchin and S. Matarrese, Phys. Rev. D **32**, 1316 (1985);  
J. J. Halliwell, Phys. Lett. B **185**, 341 (1987);  
Y. Kitada and K. -i. Maeda, Phys. Rev. D **45**, 1416 (1992).
- [71] A. R. Liddle, A. Mazumdar and F. E. Schunck, Phys. Rev. D **58**, 061301 (1998) [astro-ph/9804177].
- [72] K. -i. Maeda, Phys. Rev. D **39**, 3159 (1989).
- [73] N. Makino and M. Sasaki, Prog. Theor. Phys. **86**, 103 (1991);  
R. Fakir, S. Habib and W. Unruh, Astrophys. J. **394**, 396 (1992);  
D. I. Kaiser, Phys. Rev. D **52**, 4295 (1995);  
J. c. Hwang and H. Noh, Class. Quant. Grav. **14**, 3327 (1998).
- [74] E. Komatsu and T. Futamase, Phys. Rev. D **58**, 023004 (1998) [astro-ph/9711340];  
E. Komatsu and T. Futamase, Phys. Rev. D **59**, 064029 (1999) [astro-ph/9901127].
- [75] S. Tsujikawa and B. Gumjudpai, Phys. Rev. D **69**, 123523 (2004) [astro-ph/0402185].
- [76] R. Catena, M. Pietroni and L. Scarabello, Phys. Rev. D **76**, 084039 (2007) [astro-ph/0604492].
- [77] M. Gasperini and G. Veneziano, Phys. Rept. **373**, 1 (2003) [hep-th/0207130].
- [78] L. A. Popa, JCAP **1110**, 025 (2011) [arXiv:1107.3436 [astro-ph.CO]].
- [79] J. Ohashi and S. Tsujikawa, JCAP **1210**, 035 (2012) [arXiv:1207.4879 [gr-qc]].
- [80] S. Tsujikawa, Phys. Rev. D **85**, 083518 (2012) [arXiv:1201.5926 [astro-ph.CO]].
- [81] C. Germani and Y. Watanabe, JCAP **1107**, 031 (2011).
- [82] S. Tsujikawa and M. Sami, Phys. Lett. B **603**, 113 (2004) [hep-th/0409212].
- [83] S. Tsujikawa, Phys. Rev. D **73**, 103504 (2006) [hep-th/0601178].
- [84] N. Arkani-Hamed, H. -C. Cheng, M. A. Luty and S. Mukohyama, JHEP **0405**, 074 (2004) [hep-th/0312099].
- [85] G. Mangano, G. Miele, S. Pastor, T. Pinto, O. Pisanti and P. D. Serpico, Nucl. Phys. B **729**, 221 (2005) [hep-ph/0506164].
- [86] K. Ichikawa and T. Takahashi, Phys. Rev. D **73**, 063528 (2006) [astro-ph/0601099].
- [87] L. McAllister, E. Silverstein and A. Westphal, Phys. Rev. D **82**, 046003 (2010) [arXiv:0808.0706 [hep-th]].
- [88] E. Silverstein and A. Westphal, Phys. Rev. D **78**, 106003 (2008) [arXiv:0803.3085 [hep-th]].
- [89] C. Savage, K. Freese and W. H. Kinney, Phys. Rev. D **74**, 123511 (2006) [hep-ph/0609144].
- [90] G. R. Dvali, Q. Shafi and R. K. Schaefer, Phys. Rev. Lett. **73**, 1886 (1994) [hep-ph/9406319].
- [91] G. R. Dvali and S. H. H. Tye, Phys. Lett. B **450**, 72 (1999) [hep-ph/9812483].
- [92] J. P. Conlon and F. Quevedo, JHEP **0601**, 146 (2006) [hep-th/0509012].
- [93] S. Kachru, R. Kallosh, A. D. Linde, J. M. Maldacena, L. P. McAllister and S. P. Trivedi, JCAP **0310**, 013 (2003) [hep-th/0308055].
- [94] D. Baumann, A. Dymarsky, I. R. Klebanov, L. McAllister and P. J. Steinhardt, Phys. Rev. Lett. **99**, 141601 (2007) [arXiv:0705.3837 [hep-th]];  
D. Baumann, A. Dymarsky, I. R. Klebanov and L. McAllister, JCAP **0801**, 024 (2008) [arXiv:0706.0360 [hep-th]];  
S. Panda, M. Sami and S. Tsujikawa, Phys. Rev. D **76**, 103512 (2007) [arXiv:0707.2848 [hep-th]].
- [95] A. Linde, M. Noorbala and A. Westphal, JCAP **1103**, 013 (2011) [arXiv:1101.2652 [hep-th]].
- [96] N. Okada, M. U. Rehman and Q. Shafi, Phys. Rev. D **82**, 043502 (2010) [arXiv:1005.5161 [hep-ph]].
- [97] P. Creminelli, A. Nicolis, L. Senatore, M. Tegmark and M. Zaldarriaga, JCAP **0605**, 004 (2006) [astro-ph/0509029].
- [98] R. Maartens, D. Wands, B. A. Bassett and I. Heard, Phys. Rev. D **62**, 041301 (2000) [hep-ph/9912464];  
S. Tsujikawa and A. R. Liddle, JCAP **0403**, 001 (2004) [astro-ph/0312162].
- [99] R. Brandenberger and P. -M. Ho, Phys. Rev. D **66**, 023517 (2002) [hep-th/0203119];  
Q. -G. Huang and M. Li, JHEP **0306**, 014 (2003) [hep-th/0304203];  
S. Tsujikawa, R. Maartens and R. Brandenberger, Phys. Lett. B **574**, 141 (2003) [astro-ph/0308169];  
G. Calcagni and S. Tsujikawa, Phys. Rev. D **70**, 103514 (2004) [astro-ph/0407543].
- [100] M. Bojowald, G. M. Hossain, M. Kagan and S. Shankaranarayanan, Phys. Rev. D **79**, 043505 (2009) [Erratum-ibid. D **82**, 109903 (2010)] [arXiv:0811.1572 [gr-qc]];  
M. Bojowald and G. Calcagni, JCAP **1103**, 032 (2011) [arXiv:1011.2779 [gr-qc]];  
M. Bojowald, G. Calcagni and S. Tsujikawa, Phys. Rev. Lett. **107**, 211302 (2011) [arXiv:1101.5391 [astro-ph.CO]];  
M. Bojowald, G. Calcagni and S. Tsujikawa, JCAP **1111**, 046 (2011) [arXiv:1107.1540 [gr-qc]].